

1. Report No. TX - 96/2911-3		2. Government Accession No.		3. Recipient's Catalog No.	
4. Title and Subtitle EFFECTS OF EARLY TRAFFIC LOADING ON A BONDED CONCRETE OVERLAY				5. Report Date September 1995	
				6. Performing Organization Code	
7. Author(s) Jeffrey Lance Huddleston, David W. Fowler, and B. Frank McCullough				8. Performing Organization Report No. Research Report 2911-3	
9. Performing Organization Name and Address Center for Transportation Research The University of Texas at Austin 3208 Red River, Suite 200 Austin, Texas 78705-2650				10. Work Unit No. (TRAVIS)	
				11. Contract or Grant No. Research Study 7-2911	
				13. Type of Report and Period Covered Interim	
12. Sponsoring Agency Name and Address Texas Department of Transportation Research and Technology Transfer Office P. O. Box 5080 Austin, Texas 78763-5080				14. Sponsoring Agency Code	
15. Supplementary Notes Study conducted in cooperation with the Texas Department of Transportation. Research study title: "Full-Scale Bonded Concrete Overlay on IH-10, El Paso"					
16. Abstract  The bonded concrete overlay (BCO) is emerging as a method of pavement repair which minimizes costs and traffic disruption. When existing methods of expedited paving are combined with rapid strength gain concrete, the potential exists to return traffic on to a pavement within twenty-four hours of closure. In order to determine the long-term effects of early traffic loading on the IH-10 BCO in El Paso, Texas, a fatigue study of BCO beams was conducted. Seven beam specimens, with overlays ranging from twelve hours to seven days of age, were tested. The progression of beam deflections and cracking were monitored throughout each test to determine trends in fatigue damage with progressively younger overlays. Results indicate that rapid strength and stiffness gain in the overlay concrete minimize fatigue damage in young BCOs. Final deflections and cracking for beams loaded at twelve hours compared favorably with fully cured beams, indicating that traffic application at early ages is not detrimental to long-term pavement behavior.					
17. Key Words Bonded concrete overlays, rehabilitation strategies, early-age traffic loading			18. Distribution Statement No restrictions. This document is available to the public through the National Technical Information Service, Springfield, Virginia 22161.		
19. Security Classif. (of this report) Unclassified		20. Security Classif. (of this page) Unclassified		21. No. of Pages 96	22. Price



**EFFECTS OF EARLY TRAFFIC LOADING ON A BONDED CONCRETE  
OVERLAY**

Jeffrey Lance Huddleston

David W. Fowler

B. Frank McCullough

**Research Report 2911-3**

Research Project 7-2911

Full-Scale Bonded Concrete Overlay on IH-10 in El Paso

conducted for the

**Texas Department of Transportation**

by the

**CENTER FOR TRANSPORTATION RESEARCH**

**Bureau of Engineering Research**

**THE UNIVERSITY OF TEXAS AT AUSTIN**

September 1995



## TABLE OF CONTENTS

IMPLEMENTATION STATEMENT .....	iii
SUMMARY .....	ix
CHAPTER ONE: INTRODUCTION.....	1
1.1 Project Description.....	1
1.2 Research Objectives.....	1
1.3 Scope.....	2
1.4 Format.....	2
CHAPTER TWO: LITERATURE REVIEW .....	3
2.1 Bonded Concrete Overlay Construction .....	3
2.1.1 Background.....	3
2.1.2 Methods Of Construction.....	4
2.1.3 Design And Analysis .....	6
2.2 Early Age Considerations .....	6
2.2.1 Overlay Debonding.....	6
2.2.2 Expedited Paving .....	8
CHAPTER THREE: MIX DESIGN AND PRELIMINARY TESTING .....	9
3.1 Concrete Mix Design.....	9
3.1.1 Mix Design Requirements .....	9
3.1.2 Materials For Testing.....	10
3.1.3 Mixes Tested.....	11
3.2 Trial Mix Performance Tests .....	12
3.2.1 Compressive Strength Gain .....	12
3.2.2 Flexural Strength Gain.....	14

3.3	Mix Selection .....	15
3.4	Overlay Mix Performance Tests .....	15
3.4.1	Compressive Strength Gain .....	16
3.4.2	Modulus of Elasticity .....	16
3.4.3	Bond Performance .....	18
CHAPTER FOUR: EXPERIMENTAL PROGRAM .....		19
4.1	Purpose.....	19
4.2	Method of Implementation .....	19
CHAPTER FIVE: FATIGUE SPECIMENS .....		21
5.1	Overview.....	21
5.2	Creating the Base Beams .....	21
5.2.1	Proportioning of Size and Reinforcement.....	21
5.2.2	Formwork.....	22
5.2.3	Concrete Casting .....	23
5.2.4	Curing And Testing.....	24
5.3	Preparing the Base Beams .....	25
5.3.1	Resizing and Cutting.....	25
5.3.2	Cracking.....	26
5.3.3	Shotblasting .....	28
5.3.4	Debonding.....	31
5.4	Creating the Overlay .....	32
5.4.1	Overlay Depth.....	32
5.4.2	Formwork.....	33
5.4.3	Casting .....	33
5.4.4	Curing .....	33

CHAPTER SIX: FATIGUE TESTING PROGRAM .....	35
6.1 Testing Equipment And General Setup .....	35
6.1.1 Testing Frame .....	35
6.1.2 Load Cycling Apparatus .....	37
6.1.3 Beam Strength And Load Calculations.....	38
6.1.4 Testing Setup .....	40
6.1.5 Additional Equipment.....	43
6.2 Testing Procedures.....	44
6.2.1 Preliminary Operations .....	44
6.2.2 Operations During Fatigue Testing.....	44
6.2.3 Schedule of Testing.....	45
6.2.4 Operations After Fatigue Testing.....	46
6.2.5 Additional Tests .....	48
CHAPTER SEVEN: RESULTS OF FATIGUE PROGRAM.....	51
7.1 Static Load Deflections And Beam Cracking .....	51
7.1.1 Static Load Deflections.....	51
7.1.2 Beam Cracking.....	62
7.2 Development of Overlay Compressive Strength .....	62
7.3 Interface Bond Strength .....	65
CHAPTER EIGHT: ANALYSIS OF RESULTS .....	67
8.1 Effects Of Early Age Loading .....	67
8.1.1 Summary of Behavior Trends.....	67
8.1.2 Prediction of Deflections .....	70
8.1.3 Analysis .....	70
8.2 Interface Bond.....	72

CHAPTER NINE: SUMMARY, CONCLUSIONS, AND RECOMMENDATIONS.....	73
9.1 Summary .....	73
9.2 Conclusions From Fatigue Program .....	73
9.1.1 Early Age Loading .....	73
9.1.2 Interface Bond.....	74
9.3 Recommendations.....	74
REFERENCES .....	75
APPENDIX A: BEAM DEFLECTION DATA .....	77
APPENDIX B: BEAM CRACKING.....	83

## SUMMARY

The bonded concrete overlay (BCO) is emerging as a method of pavement repair which minimizes costs and traffic disruption. When existing methods of expedited paving are combined with rapid strength gain concrete, the potential exists to return traffic on to a pavement within twenty-four hours of closure. In order to determine the long-term effects of early traffic loading on the IH-10 BCO in El Paso, Texas, a fatigue study of BCO beams was conducted. Seven beam specimens, with overlays ranging from twelve hours to seven days of age, were tested. The progression of beam deflections and cracking were monitored throughout each test to determine trends in fatigue damage with progressively younger overlays. Results indicate that rapid strength and stiffness gain in the overlay concrete minimize fatigue damage in young BCOs. Final deflections and cracking for beams loaded at twelve hours compared favorably with fully cured beams, indicating that traffic application at early ages is not detrimental to long-term pavement behavior.



## **CHAPTER ONE: INTRODUCTION**

### **1.1 PROJECT DESCRIPTION**

Much of the national highway infrastructure constructed during the 1960s has now reached the end of its original twenty year design life-cycle. Many highways constructed later need premature rehabilitation due to the explosion of urban traffic volumes during the 1980s. The repair of these highways introduces a significant economic and logistical problem to transit departments of the nation's cities.

As these urban highways become increasingly congested, their repair and replacement becomes integrally tied with the traffic which flows along them on a daily basis. Methods of pavement rehabilitation must consider the time and extent to which commuter traffic will be disrupted. With this in mind, priority considerations of such methods necessarily include minimal lane closures, rapid lane reopening, and low overall cost. One such emerging process is the bonded concrete overlay (BCO). This technique of bonding a thin pavement overlay directly onto the original pavement has gained wider acceptance and use during the last ten years.

The Texas Department of Transportation (TxDOT) concluded that a heavily traveled section of Interstate Highway 10 (IH-10) through downtown El Paso, Texas represents a prime candidate for employing this BCO technique (Ref 1). This pavement, originally built in 1965, is still in relatively good condition but needs updating to meet current and future traffic loads. In order to fully consider and evaluate all options available for the design and construction of the overlay, TxDOT initiated a joint research project. The project partners include The Texas Department of Transportation (TxDOT), The Federal Highways Administration (FHWA), and The Center for Transportation Research (CTR). The three-year study will culminate in the complete reconstruction of 1.28 km of the six-lane divided highway through downtown El Paso.

### **1.2 RESEARCH OBJECTIVES**

While the ultimate goal of this project lies in the actual design and construction of the BCO, several others related topics require detailed investigation. The complete objectives of this project therefore include:

1. Evaluation of existing pavement conditions and determination of required overlay thickness.
2. Development of overlay concrete mix design.
3. Testing of concrete properties such as strength, modulus, thermal coefficient, and shrinkage.
4. Evaluation of concrete bond development and performance.
5. Testing and evaluation of BCO fatigue performance at early ages.
6. Determination of construction sequence and timing for rapid reopening.
7. Development of construction guidelines for acceptable BCO placement.
8. Construction and monitoring of test sections for evaluation of various construction factors.
9. Construction and long term monitoring of the BCO highway.

### **1.3 SCOPE**

The scope of research, testing, and results presented in this report include only a portion of the overall project objectives. Specifically, this report will address:

1. Concrete overlay mix design and testing of associated properties.
2. Testing and evaluation of BCO fatigue performance at early ages.
3. Evaluation of interface bond capacity with respect to early loading.
4. Recommendations concerning early age traffic loading.

### **1.4 FORMAT**

The major conceptual divisions of this report are separated into chapters for individual discussion. This first chapter introduced the report topic and presented the research goals. Chapter Two contains background information on BCO construction and it's related topics. Chapter Three presents the overlay mix design and preliminary strength testing. Chapter Four briefly identifies the proposed testing program. Chapter Five describes preparation of the fatigue testing specimens. Chapter Six outlines the testing procedures and apparatus utilized during the fatigue testing program. Chapter Seven presents the testing results. In Chapter Eight these results are discussed and analyzed. Chapter Nine details the conclusions drawn from the research and presents recommendations for the future. Finally, the Appendix includes the data from the testing program.

## **CHAPTER TWO: LITERATURE REVIEW**

### **2.1 BONDED CONCRETE OVERLAY CONSTRUCTION**

The repair of deteriorating concrete roadways has traditionally focused on two contrasting techniques of reconstruction. Pavements can either be completely replaced or rebuilt through a combination of patching and overlays. While sometimes necessary for severely damaged pavements, full depth reconstruction is often costly, time consuming, and traffic obstructing. The common alternative relies on making minor repairs, such as sealing cracks and spalls, and then overlaying the original roadway with a new wearing surface. Due to its low initial cost and ease of rapid application, asphalt concrete is usually the material of choice. As traffic volumes have rapidly increased, however, the short life of the asphalt overlay has made this alternative less economical and desirable. With these considerations, transportation departments around the country are looking to a third alternative, the bonded concrete overlay (Ref 2). The following chapter provides background information on important topics and relevant research concerning BCOs.

#### **2.1.1 Background**

The term “bonded concrete overlay” merely indicates that the newly placed concrete traveling surface acts in full composite action with the original roadway instead of forming a new and separate layer. In one fashion or another, this repair concept has existed since the turn of the century. The earliest applications did not consider the behavioral mechanisms involved with forming a new composite roadway. A thin layer of concrete was simply laid down and finished to create the new traveling surface. In later experimental projects, an effort was made to enhance the bond by cleaning the road surface and applying cement grout immediately before concrete overlay placement (Ref 3).

While some laboratory research and experimental roadways were conducted during the 1930s and 50s, it was not until the late 1970s that major modern research into BCO mechanisms began. Notable projects include the 1977 Iowa Department of Transportation construction of a 2.1-km experimental overlay. Factors such as overlay thickness, reinforcement, and base surface

preparation were varied throughout the project. Delaminations were noted in zones of secondary joint cracking (Ref 3). A 1981 test section on IH-80 in California developed serious debonding problems due to severe environmental conditions and was subsequently replaced with an asphalt concrete overlay (Ref 3).

The Texas Department of Transportation (TxDOT) has undertaken several BCO projects in the last decade. Beginning in 1983, the IH-610 loop around downtown Houston was used as a major testing location for three BCO projects to rehabilitate the continuously reinforced pavement. The first consisted of a four-lane, 500-m section on the south loop (Ref 4). The 5.08- and 7.62-cm-thick sections involved various types of reinforcement, including wire mesh and steel fibers. The success of this test led to a major follow-up project in 1985 (Ref 5). A total lane length of forty-five km was paved with a 10.16-cm overlay on the north loop. Subsequent road surveys revealed minor overall delaminations with some higher occurrences in localized areas. In 1990 the program returned to the south loop for the placement of sixty-four km of bonded concrete overlay. Again, reinforcement and placement methods varied to allow for study of several sub-sections. One test section was replaced after major debonding occurred within the first twenty-four hours. The latex grout applied prior to overlay placement dried prematurely and formed a debonding layer instead of enhancing overlay bond. Other sections performed well and continue to be monitored for long term behavior (Ref 6).

### **2.1.2 Methods Of Construction**

Actual placement of a BCO simply involves laying the overlay concrete and finishing the traveling surface. However, preparation of the base roadway, types of overlay reinforcement, and methods of curing can vary significantly. Current research projects often include variations of each factor in order to collect data on their combined effects.

Early efforts at base preparation involved a minimalist approach of wet brooming the surface and applying a film of cement grout. As later research identified the need for a more positive connection between the base and overlay, methods of increasing the base surface texture were developed. Techniques include cold milling, sandblasting, hydrocleaning, and shotblasting. Projects such as the 1983 Houston overlay utilized a combination of cold milling and

sandblasting to remove the weak top laitance and create a new roughly textured surface. However, planes of aggregate fracture created by the cold milling process tended to reduce overall bond capacity in localized regions. The modern techniques of hydrocleaning and shotblasting roughen the concrete surface by bombarding the paste with water or steel shot. When used at a proper application rate, as in the 1990 Houston overlay project, both methods enhance the texture to create increased surface area for bonding and interlock with the overlay concrete (Ref 5).

Numerous types of reinforcement have been employed in BCO research projects. Some test sections have been unreinforced, but most used either reinforcing steel, welded wire mesh, or steel fibers. A study on the effects of interface conditions concluded that for thin overlays the rebar and mesh could lie directly at the interface without reducing bond (Ref 7). Eliminating steel chairs allows for simpler and faster placement. The use of steel fibers in the overlay concrete has been considered as both a supplement and replacement to traditional reinforcement. Since the primary purpose of overlay reinforcement is to control shrinkage and thermal cracking, a dispersion of steel fibers presents an attractive alternative. Elimination of overlay reinforcement bars would simplify construction and greatly reduce labor costs. A recent experimental roadway near El Paso, Texas included sections with rebar, steel fibers, and both combined. Preliminary testing results reveal little or no difference in performance between the traditional and fiber reinforced sections (Ref 8).

Proper curing of the overlay is critical to both immediate and long term performance of a BCO. Water and oil based curing compounds help retain moisture to ensure proper hydration and achievement of overlay design strengths (Ref 9). During the first forty-eight hours after placement, this water retention minimizes volume changes which reduces plastic shrinkage cracking. At low application rates, these spray compounds become ineffective because moisture can travel horizontally and escape through uncovered areas. Alternatives include the use of wet burlap mats or plastic sheeting. These are generally more labor intensive and their removal after four to seven days provides for less long-term hydration than the long wearing curing compounds.

### **2.1.3 Design And Analysis**

The design of a BCO pavement thickness necessarily includes the standard input such as predicted traffic volumes and desired life span. However, because the overlay thickness design relies on the integral behavior of the base and overlay, the base roadway condition must be taken into account. Depending on the extent of cracking and damage, the actual base pavement can be converted into an equivalent new pavement thickness for use in calculating the necessary overlay thickness (Refs 10,11). This remaining life concept provides that as a base pavement's condition deteriorates, the required overlay thickness increases to compensate for a loss of effective thickness. At the lower bound, a severely damaged base roadway provides no structural contribution. Here, no attempt is made to develop bond and the overlay accounts for the entire design. The remaining life of a pavement can be determined through a mechanistic fatigue model or by assessing the current state of distress through road surveys and past loading history.

Several pavement design guidelines exist for calculating the overlay pavement thickness required for a given set of conditions. Standard guidelines, such as AASHTO Guide for Design of Pavement Structures, use empirical design equations to calculate the necessary total pavement thickness. The overlay thickness is then obtained by subtracting the effective thickness of the existing pavement, as determined by remaining life analysis. Other computerized programs such as Pavement Rehabilitation Design System (PRDS), developed by CTR, rely on a mechanistic design using large sets of accurate data input to directly formulate an overlay thickness (Ref 1).

## **2.2 EARLY AGE CONSIDERATIONS**

Surveys of previous experimental BCO roadways show that the long- term performance depends heavily on initial conditions (Ref 3). BCOs which do not show signs of distress during the first months after placement will generally not develop major problems such as debonding in later years. However, overlays which substantially debond at early ages will incur larger traffic stresses which can significantly reduce their fatigue life expectancy.

### **2.2.1 Overlay Debonding**

Signs of debonded overlays on previous experimental projects have typically become evident within days or weeks of placement. Debonding of the latex-grouted section of IH-610

South in Houston was noticed within twenty-four hours. This early age debonding has been linked to a combination of factors.

Debonding occurs when interface stresses exceed the bond capacity developing between the base surface and overlay concrete. The first forty-eight hours are most critical because the overlay can experience its highest lifetime stress at a time when bond is weakest and still maturing. Stresses are induced at the interface through both tension and shear. The causes of stress, besides traffic loading, involve differential volume changes and differential temperatures between the attached overlay and base. These effects alone can cause interface stresses in the range of 290 kPa (Ref 11).

Interface bond can develop rapidly as the overlay gains strength. Tests by Wade at the University of Texas show that by twenty-four hours of age bond can reach 2,575 kPa (Ref 12), well above the critical stress range. The key is to provide conditions in which this development can occur. Proper concrete curing, through spray compounds or wet mats, ensures hydration and strength gain. Improper preparation of the base surface, however, can severely limit the ultimate bond strength. Surface roughening increases bond capacity by creating additional bond surface area and forming a field of aggregate interlock. Roughness can be measured with the sand patch test (Ref 5). Once this relative indicator has been linked to good bond through lab testing, a simple field test will verify that measures such as shotblasting or hydrocleaning have achieved desirable results.

Methods of preventing overlay debonding at early ages rely on keeping stresses lower than the developing bond capacity. Water evaporation in the overlay causes a volume reduction relative to the base which produces an interface stress. Evaporation rates above  $1.0 \text{ kg/m}^2/\text{hr}$  are likely to produce serious problems (Ref 6). By placing the concrete during conditions with cooler temperatures, low winds, and higher humidity, evaporation can be minimized. Timely placement of surface spray compounds also helps. Large temperature swings in the concrete can also cause interface stresses. These variations can be minimized by reducing the concrete heat of hydration and placing concrete at night so that initial temperature buildup in the overlay does not correlate with high day time air temperatures.

### **2.2.2 Expedited Paving**

The term “expedited paving” refers to a process whereby roadway construction and traffic return is accomplished during the shortest possible time period. Expedited paving has become an important goal in order to minimize expensive traffic congestion and disruption (Ref 1). The bonded concrete overlay represents an excellent method of achieving such goals. When compared with standard construction techniques, the BCO can be achieved in shorter time spans. Surface preparation of an existing pavement generally requires far less effort and time than full depth base work. Development of overlay concrete mixes which can withstand application of traffic at very early ages would make the overall BCO process very expedient and allow for minimal traffic disruptions. However, the effect of traffic stresses on very young BCOs are unknown and research is needed to determine their effect on long-term behavior. Previous fatigue studies of long-term BCO behavior, such as that by Riley (Ref 13), focused primarily on remaining life concepts of the base and fully cured overlay.

## CHAPTER THREE: MIX DESIGN AND PRELIMINARY TESTING

### 3.1 CONCRETE MIX DESIGN

Before any testing of the bonded concrete overlay behavior could begin, the concrete mix design had to be developed. Several different mixes were tested using a variety of mix constituents and proportions. Each mix was then evaluated on the basis of strength gain properties, workability, and overall cost.

#### 3.1.1 Mix Design Requirements

According to American Concrete Institute (ACI) mix design guidelines (Ref 14), the maximum size of course aggregate allowed in a paving mix is one-third the slab thickness. Initial estimates of the overlay thickness focused on an approximate value of 7.62 cm. This in turn dictated that the maximum course aggregate size be 2.54 cm or less. The TxDOT standard course aggregate grade #6 was thus the largest deemed acceptable for the overlay mix.

Further restrictions on mix designs intended for overlay use are dictated by current TxDOT specifications (Ref 15). These requirements are intended as a basis for guiding the designer to provide a certain degree of uniformity in pavement characteristics. The overlay mix specifications are listed in Table 3.1.

**Table 3.1. Overlay Mix Specifications**

Minimum 28-day compressive strength	31,700 kPa
Minimum 7-day flexural strength	4,400 kPa
Minimum cement content	3802 N/m <sup>3</sup>
Maximum water to cement ratio	0.40
Maximum slump	12.7 cm
Desired paving slump	3.8 cm
Entrained air content	6% ± 1.5%
Maximum course aggregate size	TxDOT grade #6

### 3.1.2 Materials for Testing

Due to concerns of cost and availability, aggregates from quarries in the El Paso region were chosen for employment in the BCO mix. Samples of the local sand and rock were shipped to the CMRG laboratory for use in the mix and testing processes. Initially, TxDOT proposed utilizing a blend of the two most common course aggregate gradations which were locally available and met TxDOT gradation specifications. These two types were the grade #467, a 3.8-cm-minus crushed limestone, and grade #67, a 1.9-cm-minus crushed limestone. The local grade #67 fulfilled the specifications of the grade #6 previously specified. After consideration of the possible overlay thickness, it was concluded that the #467 aggregate would not meet the one-third dimension rule for workability. This type was thus eliminated from consideration, leaving the grade #67 as the only course aggregate. Aggregate properties are summarized in Table 3.2.

**Table 3.2. Aggregate Properties**

	<b>Course Aggregate</b>	<b>Fine Aggregate</b>
Type	Crushed dolomitic limestone	local sand
Bulk Specific Gravity (BSG)	2.70	2.60
Dry Rodded Unit Weight (DRUW)	510 kN/m <sup>3</sup>	
Fineness Modulus (FM)		2.80

Two types of cement were originally tested in the mix design process. A type I/II standard Portland Cement produced in El Paso was provided by Jobe Concrete. The use of a local cement was deemed important for minimizing possible delays and overall mix costs. The second cement type considered was Pyrament®. Pyrament is a blended cement produced by Lone Star Industries which is available with set times of 30, 60, and 90 minutes. Concrete using Pyrament tends to reach extremely high early strengths, and is used for patchwork and airplane runway replacement. A third alternative, a local type V low heat of hydration cement, was not considered during this testing program but will be evaluated at a later date.

In order to meet the air content, strength, and workability requirements, the use of admixtures was necessary (Ref 16). For air content, Grace Darex II® air entraining admixture was utilized. Two types of superplasticizer were tested for their ability to increase workability, reduce the required water content, and increase early age strength. Rheobuild® 1000, a high range water reducer, and Polyheed® 997, a medium range water reducer, were provided by Master Builders Co.

### 3.1.3 Mixes Tested

Three primary types of concrete mix were tested. As a basic reference, the first mix utilized standard proportions suggested by ACI paving mix design procedures. The second type of mix, involving superplasticizers, was designed using the characteristics of the first mix as a reference. The cement content was increased, water to cement ratio decreased, superplasticizers added, and aggregate proportions varied for workability. Both the Rheobuild®1000 and Polyheed® 997 additives were tested. Since the dosage rate for Polyheed turned out to be significantly higher than Rheobuild without corresponding strength increase, this mix was eliminated early in the testing program. The third type of mix involved the blended Pyrament® cement and mix proportions suggested by the manufacturer. All final mix proportions were composed utilizing the absolute volume method (Ref 14). Table 3.3 shows the final mix constituents for each of the three mixes tested. Table 3.4 indicates the important mix parameters.

**Table 3.3. Constituents of Three Mixes Tested**

	<b>Basic</b>	<b>Rheobuild</b>	<b>Pyrament</b>
<i>Mix Constituents</i>	<i>Weight, N/m<sup>3</sup></i>		
Water	1,484	1,478	920
Type I/II Cement	3,713	5,098	-
Pyrament Cement	-	-	4,377
Fine Aggregate	6,605	6,402	8,014
Course Aggregate			10,988

<i>Admixtures</i>	<i>Volume, ml/100N of cement</i>		
Darex II		26.6	-
Rheobuild® 1000	-	8.0	-

**Table 3.4. Important Mix Parameters**

	<b>Basic</b>	<b>Rheobuild</b>	<b>Pyrament</b>
Water/Cement Ratio	0.4	0.29	0.21
Cement Content N/m <sup>3</sup>	3,719	5,098	4,387
Water Content ml/N	40.7	29.9	21.5
Initial Slump cm	2.5-7.6	1.2-2.5	0
Final Slump cm	2.5-7.6	12.7-18	12.7-18
Air Content	6%	5%	2.5%

### 3.2 TRIAL MIX PERFORMANCE TESTS

Samples were taken from each concrete mix batch for the purpose of testing strength development. Curing conditions varied slightly depending on the weather conditions. Generally, cylinders and beams were cured outside under wet burlap and plastic sheeting for three to seven days. Specimens were then demolded and placed in a chamber of lime-saturated water at 21°C until twenty-eight days. This two-stage curing process was an attempt to obtain early age strengths similar to those which might be encountered in the field. Curing specimens by ASTM C192 specifications (Ref 17) would have significantly underestimated the early age strength gain occurring in the hot summer climate of El Paso.

#### 3.2.1 Compressive Strength Gain

Compressive strength tests were performed on 10.2- by 20.3-cm cylinder specimens according to the ASTM C39 method (Ref 17). A Forney Cylinder Testing Machine with a 2,700-kN capacity was utilized. Loading proceeded at 175 kN per minute. Cylinder strengths

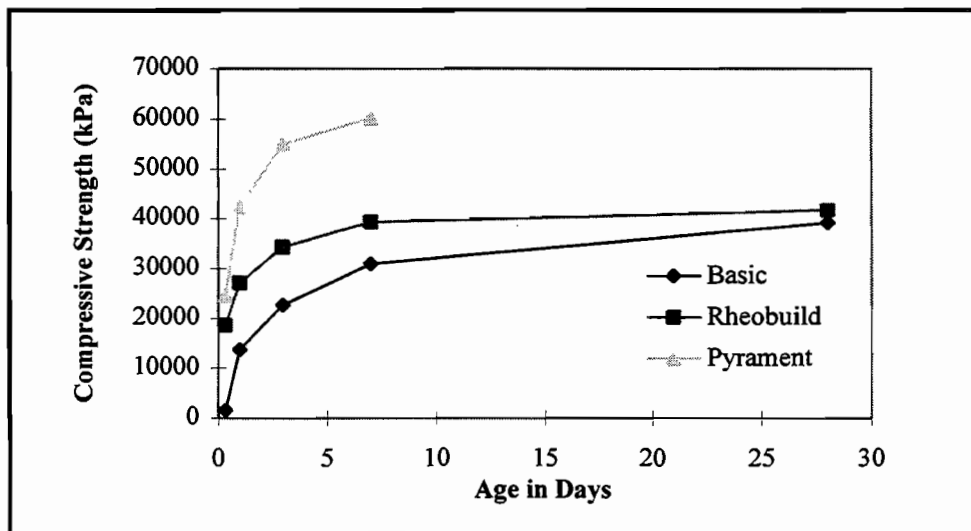
were tested at 8 hours, 1 day, 3 days, 7 days, and 28 days in order to obtain a complete strength gain curve.

Table 3.5 shows the cylinder strengths for each of the three trial mixes tested. The same data are presented graphically in Figure 3.1. Clearly, all mixes meet and exceed the specified 28-day compressive strength of 31,700 kPa. At the critical early ages, however, the Rheobuild and Pyrament mixes surpass the base mix in strength gain.

**Table 3.5. Compressive Strength Development of Trial Mixes in kPa**

Age (days)	Basic	Rheobuild	Pyrament
0.33	1,500	18,600	24,700
1.0	13,700	27,100	42,300
3.0	22,700	34,200	55,000
7.0	30,900	39,300 <sup>a</sup>	60,200
28.0	39,100	41,600 <sup>a</sup>	-

<sup>a</sup> Strength gain reduced due to dry curing conditions



**Figure 3.1. Compressive Strength Development of Trial Mixes**

### 3.2.2 Flexural Strength Gain

Flexural strength tests were performed on 15.2- by 15.2- by 53.3-cm beam specimens according to the ASTM C78 method (Ref 17). A Reinhart Beam Testing Machine with a three-point loading setup was utilized. Loading proceeded by following the curved rate path on the standard testing sheets. Beam strengths were tested at 8 hours, 1 day, 7 days, and 28 days in order to obtain a complete strength gain curve.

Table 3.6 shows the beam strengths for each of the three trial mixes tested. The same data are presented graphically in Figure 3.2. The basic mix did not meet the required flexural strength of 4,400 kPa within the first seven day period. The Rheobuild and Pyrament mixes, however, reached the specification after one day of curing. At seven days both these mixes greatly surpassed the required strength. The apparent drop in flexural strength of the Rheobuild mix after twenty-four hours was due to testing error. Thermocouples for measuring concrete maturity were mistakenly placed in the central third of the beam instead of closer to the end. During the third-point flexural testing, these beams broke prematurely at the weakened location caused by the thermocouples. As exemplified by the basic and Pyrament mixes, substantial hydration was still proceeding through at least seven days of age. Since the one-day strength already exceeded specifications, additional flexural testing was left for a later date.

**Table 3.6. Flexural Strength Development of Trial Mixes in kPa**

<b>Age (days)</b>	<b>Basic</b>	<b>Rheobuild</b>	<b>Pyrament</b>
0.33	690	3,680	3,790
1.0	3,680	4960	5,740
7.0	4,140	4,620 <sup>a</sup>	7,360
28.0	4,930	4,140 <sup>a</sup>	7,590 <sup>b</sup>

<sup>a</sup> Premature breaks caused by thermocouple wires embedded in specimens

<sup>b</sup> Flexural strength actually higher than charts able to measure

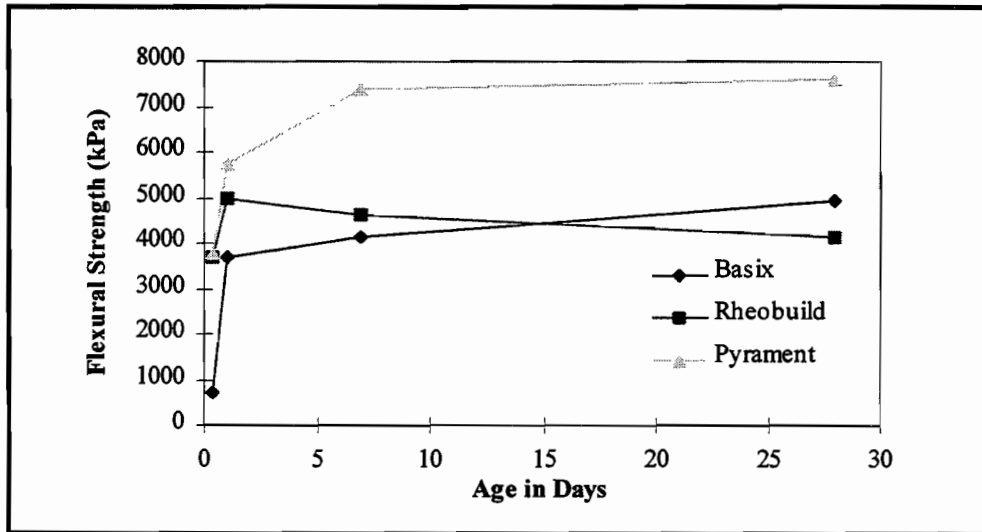


**Figure 3.2. Flexural Strength Development of Trial Mixes**

### 3.3 MIX SELECTION

The final selection of a mix design for the overlay involved the factors of strength gain and cost. The standard TxDOT mix, with some slight alterations, would meet the required strength specifications. However, the Rheobuild® and Pyrament® mixes both showed greatly enhanced strength gain in the critical first days. The estimated costs of the basic, Rheobuild, and Pyrament mixes are \$79, \$94, and \$165 /m<sup>3</sup>. The high cost of the Pyrament cement was considered a significant drawback even though it showed the best strength gain. Thus, for reasons of strong early age strength and moderate cost, the Rheobuild mix design was recommended and subsequently chosen for use in the bonded concrete overlay.

### 3.4 OVERLAY MIX PERFORMANCE TESTS

Once the Rheobuild mix was selected for use in the BCO, further mix batches were made in order to obtain data on the behavior and strength gain. Besides additional compressive strength tests, modulus of elasticity tests were performed and the shear bond capacity was investigated.

### 3.4.1 Compressive Strength Gain

Using the same methods and procedures as previous described, the compressive strength of the overlay mix was tested at 1, 2, 3, 5, 7, and 28 days. The complete twenty-eight day strength gain is charted in Figure 3.3. The early age strengths compare favorably with the preliminary test results. Later ages show sizable increases, with twenty-eight day strengths reaching 49,030 kPa compared to 41,630 kPa in the trial mixes. This effect is due solely to proper curing procedures being observed.

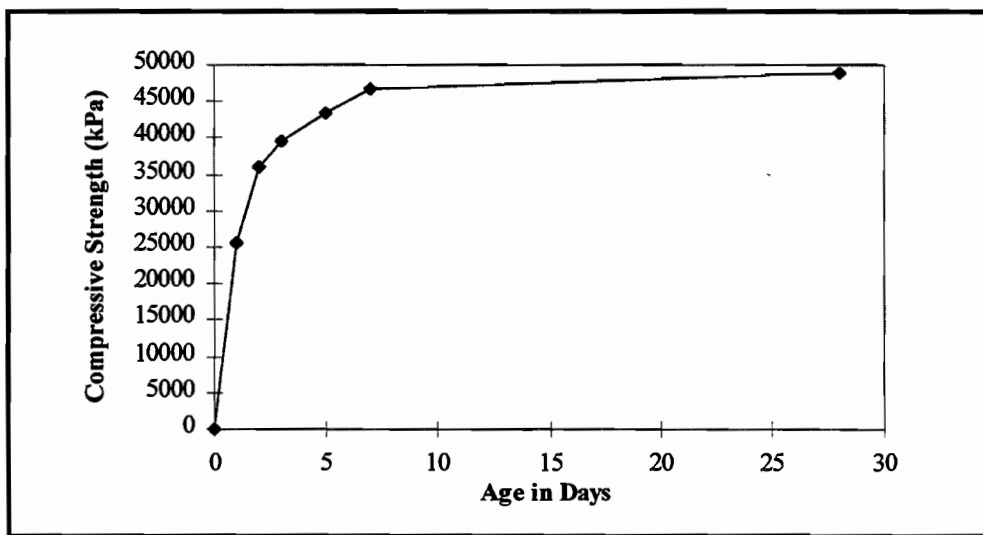


**Figure 3.3. Compressive Strength Development of Overlay Mix**

### 3.4.2 Modulus of Elasticity

In order to provide information on the stiffness of the overlay mix for the pavement design process, modulus of elasticity tests were performed along with the compressive strength tests. ASTM C469 modulus testing procedure was followed (Ref 17). Cylinder specimens were placed in a swing-arm style compressometer (with a 14.0-cm gauge length) and loaded in the Forney compression testing machine. At increments of load up to 40% of the concrete ultimate compressive strength ( $f'c$ ), deflection readings were taken. These data were then converted to

stress and strain and plotted for each cylinder. Modulus values were calculated using the tangent offset method. Final values of modulus represent the weighted average of three specimens.

In Table 3.8 the values of compressive strength, modulus, and correlation factor are given for each age. The modulus reached a value of  $38.4 \times 10^6$  kPa at twenty-eight days in this particular batch. Other batches of this mix routinely reached compressive strengths of 55,000 kPa and moduli of  $40.1 \times 10^6$  kPa. Ambient curing temperature affected the rate of gain during the twenty-eight day period. The correlation factor represents the integral relationship between compressive strength and modulus for concrete (Ref 18). Equation 3.1 illustrates this simple relationship.

$$E = C.F. \cdot \sqrt{f'c} \quad \text{Eq. 3-1}$$

where E = concrete modulus of elasticity, kPa  
 f'c = compressive strength of concrete, kPa  
 C.F. = numerical correlation factor

While ACI 318 indicates a typical value of 149,670 for C.F., the overlay mix tested produced a range from 167,500 to 177,870 with an average value of 170,950. This correlation factor allows those monitoring the pavement to accurately determine the pavement stiffness from compressive strength specimens taken during the paving process.

**Table 3.7. Compressive Strength and Modulus of Overlay Mix**

Age (days)	Compressive Strength (kPa)	Modulus of Elasticity (kPa)	Correlation Factor
1	25,600	$28.5 \times 10^6$	177,870
2	36,100	$33.1 \times 10^6$	174,850
3	39,700	$33.8 \times 10^6$	168,660
5	43,400	$35.0 \times 10^6$	167,500
7	46,600	$37.0 \times 10^6$	170,390
28	49,000	$38.4 \times 10^6$	173,640

### 3.4.3 Bond Capacity

The shear bond strength of a bonded concrete overlay is critical to the pavement performance. This is especially true at early ages when high thermal and shrinkage stresses occur in the overlay. In order to make an initial assessment as to the bond capability of the overlay mix, shear bond tests were performed using the shear block pull-off test. Wade performed more comprehensive shear tests using a guillotine shear apparatus (Ref 12).

The shear block test used was developed by Choi at the University of Texas at Austin (Ref 19). In this test, bond strength is determined by horizontally shearing an overlay block from the roughened base block it is cast upon. A system of bearing plates and hydraulic rams is utilized to direct the shear force along the interface plane. For the guillotine shear test, a 10.16-cm cylinder or core is used. The base of the cylinder is held horizontally in the guillotine frame while a loading block acts vertically upon the unsupported overlay side of the interface. The complete details of both procedures are described by Wade (Ref 12). Bond readings were taken at 8, 24, and 48 hours. The bond test results in Table 3.8 indicate that even at eight hours this mix has sufficient capacity to resist thermal and shrinkage effects. Previous research indicates that the maximum stresses reached early in the life of a pavement are in the range of only 290 kPa (Ref 3).

**Table 3.8. Bond Capacity of Overlay Mix**

<b>Overlay Age (Hours)</b>	<b>Shear Block Bond Strength (kPa)</b>	<b>Average Guillotine Bond Strength (kPa)</b>
8	852	1720
24	3123	2575
48	2666	3380

## **CHAPTER FOUR: EXPERIMENTAL PROGRAM**

### **4.1 PURPOSE**

The experimental program set forth in Chapters Five and Six was developed for the express purpose of determining the effects of early age traffic loading on the bonded concrete overlay mix design presented in Chapter Three. The effects of early traffic loads require study to provide information for two critical areas of concern in the El Paso project: (1) the earliest time after casting that traffic be allowed back on the highway and (2) the effect of this early traffic flow on the expected lifespan of the fresh overlay pavement. The information gained from this experimental program will be studied in correlation with other project research to answer these crucial questions

### **4.2 METHOD OF IMPLEMENTATION**

After reviewing the literature and previous research presented in Chapter Two, a method of implementing the experimental program was selected. The dominating factors included time dependent loading and life-time behavior. In order to observe the effects of traffic loads on a freshly placed BCO, a number of specimens at various ages needed to be tested. By beginning with fully cured specimens and then testing ones with progressively younger overlays, a trend in behavior could be established. The short time-span available for laboratory testing obviously dictated a program involving accelerated load application such as cyclic fatigue testing. Determining the exact type of loading setup and fatigue specimen, however, required careful consideration.

As discussed in Chapter Two, similar research on the fatigue behavior of bonded concrete overlays by Riley (Ref 13) focused on replicating small portions of a BCO pavement and substrate to achieve an accurate testing simulation. As such, the program involved half-scale bonded overlay slabs fully supported on neoprene pads for duplication of the in-situ base conditions. Because the slabs were more resistant to fatigue loading than expected, an increase in the applied loading from 22.24 kN to 88.96 kN was required to cause failure within the 2,000,000 load cycle test parameter. Since effects of pavement loads increase exponentially (Ref

11), this four-fold increase in applied fatigue load equaled over a sixty-fold increase in effective loading cycles.

This greatly accelerated method of achieving failure causes internal stresses which a real pavement would never experience. The effects upon critical regions such as the bonded interface and young overlay concrete might produce results contrary to a normal lifetime of traffic. For these reasons, testing a supported slab which might require large fatigue loads was deemed undesirable. A simpler system with loads closer to actual vehicle traffic was needed.

Instead of a fully-supported slab, a simply-supported beam was selected as the testing specimen. Because beams lack the support base provided to a true pavement, a direct application of resulting data will not be feasible. However, behavior variations among the beam test specimens could be analyzed for trends and meaningful indicators. The results of this analysis could then be interpreted for application to the actual overlay project. Using such an element presented four distinct advantages over supported slabs:

1. A determinate testing system allows for direct calculation of member stresses and analysis of results.
2. Simply supported test specimens require application of lower load levels to cause distress and failure.
3. With a simply-supported setup, the fatigue failure load can be predetermined within ten to fifteen percent.
4. Casting smaller beam members requires less time, allowing for testing of additional specimens to produce more conclusive results.

The specifics of the BCO fatigue beam specimens fabrication are presented in Chapter Five. The actual setup and procedures of the fatigue testing program are presented in Chapter Six.

## **CHAPTER FIVE: FATIGUE SPECIMENS**

### **5.1 OVERVIEW**

In order to determine the effects of early age loading on the bonded concrete overlay, a fatigue testing program was developed. Details of the fatigue specimen preparation are outlined in the following sections. In Chapter 6 the actual testing program and apparatus are discussed.

Development of the overlay beams for the fatigue testing program consisted of three primary steps. In the first, the base beams were cast and then allowed to cure for a significant period of time. For the second procedure, preparation work was done to the base beams. In the final step, the new overlay mix was cast upon the base beams to create the complete fatigue specimen.

### **5.2 CREATING THE BASE BEAMS**

At the commencement of this project, a general time line of activities was charted. From this time line, the immediate need for casting base slabs for the fatigue program was realized. This urgency rested on the length of time needed to cure the slabs before additional work could proceed. Since this casting process was to proceed before extensive literature review and mix testing had been conducted, some assumptions were made which needed to be corrected later.

#### **5.2.1 Proportioning of Size and Reinforcement**

The base beam dimensions and reinforcing were originally selected for the concept of testing a half-scale model of a slab section from IH-10 in El Paso. As such, the planar dimensions were selected as 0.914 m wide by 1.829 m long. These dimensions were considered adequate for any intended usage and the maximum which could reliably fit into the testing frame available at CMRG. These initial choices relied heavily upon similar fatigue research performed by Riley at The University of Texas (Ref 13).

The actual pavement in El Paso was cored at numerous locations in order to determine the in-situ thickness. Results of these tests indicated the pavement thickness varied from 19.1 cm to 24.8 cm with a mean value of 20.9 cm. Thus, at half-scale the base slab was required to be 10.4 cm thick. As a simpler working value, 10.2 cm (4.0 in.) was chosen.

A review of the original 1960 construction specifications, supplied by TxDOT, revealed that the longitudinal and transverse reinforcing consisted of #5 bars at 19.1 cm and #4 bars at 76.2 cm, respectively. At a 20.3-cm thickness, this equated to a reinforcing percentage of 0.52% and 0.083% for each direction. As the slab dimensions scale down, these percentages remain the same. At a half-scale 10.2 cm thickness the slab steel required in the longitudinal direction was 5.60 cm<sup>2</sup>/m of width. In the transverse direction, 0.85 cm<sup>2</sup>/m of length was needed. For ease of construction, #3 size (0.95 cm diameter) standard deformed reinforcing steel bars were utilized. From the calculated reinforcing ratios, the equivalent longitudinal steel spacing was determined to be 12.7 cm and the transverse spacing 83.8 cm.

### **5.2.2 Formwork**

The reinforcing steel was ordered from a local supplier pre-cut to lengths of 2.438 m and 0.864 m. These lengths differed slightly from the actual cast slab dimensions. This was done so that the transverse steel would easily fit within the formwork and the longitudinal steel could extend through the formwork for support and potentially access at later times.

The formwork for casting the base slabs consisted of 3.81-cm-thick construction grade lumber cut to the slab dimensions and bolted together to create a rectangular frame. Laminated plywood, 0.635 cm thick, was screwed to the frame's bottom to complete the formwork. Holes were drilled at a 12.7-cm spacing at midheight of the end lumber. This allowed the longitudinal reinforcing to extend through the formwork and rest securely at the ends. The transverse steel was tied to longitudinal bars in order to prevent spreading during the concrete pour. Twelve such forms were prepared. This layout is illustrated in Figure 5.1. The method of formwork construction allowed for simple removal by unscrewing the base plywood and framework, then slipping the end forms from the steel threaded through them.

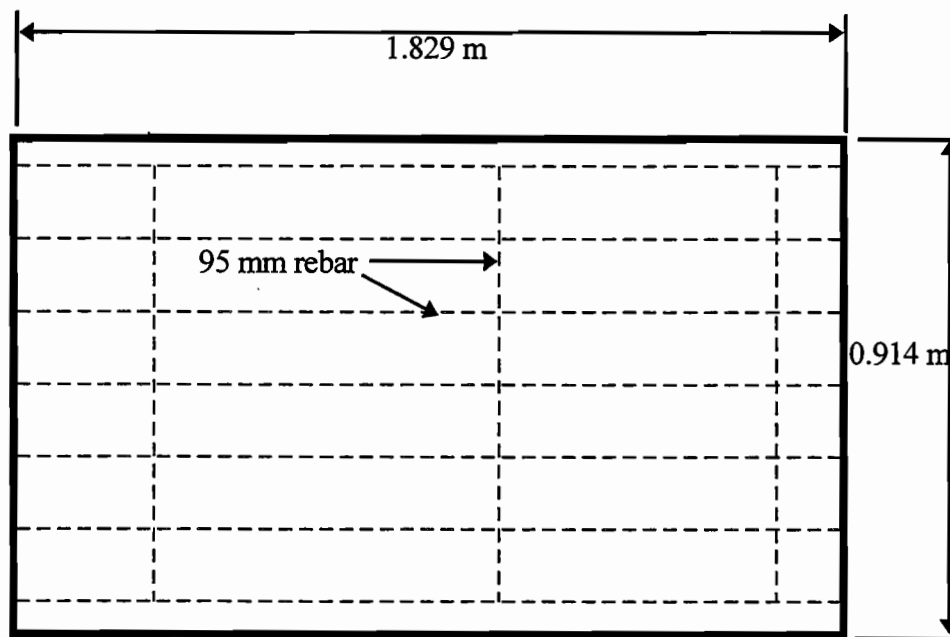


**Figure 5.1. Layout of Base Slab Reinforcing**

### 5.2.3 Concrete Casting

Ideally, the concrete batched for the base slabs would have matched the existing pavement in El Paso. Due to the volume of concrete required for the base slabs, however, the mix could not be batched by hand utilizing the local materials. Also, the 10.16-cm slab thickness precluded employing the 3.81-cm aggregate actually found in the pavement. Instead of trying to match the mix constituents, the concrete was specified only by desired strength and maximum permissible size of course aggregate. The strength of the pavement was determined from cores and an equivalent mix developed by Capitol Aggregates, a local ready-mix company. The cores previously tested for compressive strength produced values ranging from 35,504 kPa to 56,462 kPa. The median value of 44,120 kPa was used as the target strength for the base slab mix.

The concrete mix was delivered to the work site in a 6.88 m<sup>3</sup> capacity ready-mix truck. After pre-oiling the wooden forms, the concrete was shoveled into place and consolidated with a 2.54 cm needle nose vibrator. The top surface of the slabs was struck off with a wooden plank

and then smoothly finished with a metal hand trowel. In Figure 5.2 a stack of the cured slabs are shown after they were removed from their formwork.

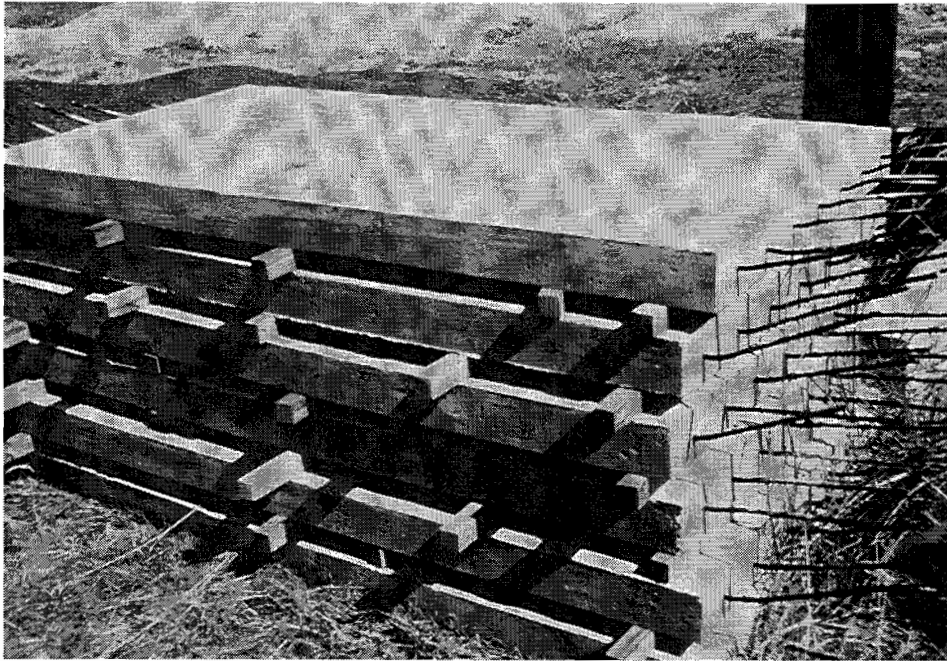


**Figure 5.2. Base Slabs After Formwork Removal**

#### **5.2.4 Curing and Testing**

During the process of casting the base slabs, samples of concrete were taken in order to cast testing specimens. A total of twenty-four cylinders and eight flexural beams were cast according to the ASTM procedures previously discussed. These specimens were placed adjacent to the base slabs so as to receive the same moisture and temperature environment.

For the first seven days after slabs were cast, the test specimens and the base slabs were kept moist with wet burlap and sealed with a covering of plastic sheeting. This was done in order to ensure proper curing and strength gain. After seven days, the burlap was removed, and the concrete was left to cure for an indefinite length of time. Instead of placing the test specimens in the standard ASTM curing environment for the remainder of the first twenty-eight



days, they were left with the base slabs so as to undergo similar curing and more closely simulate the actual concrete strength.

After seven days of curing, two flexural beams were removed from the field and tested to give an indication of the mix capacity. The beam strength averaged 3,790 kPa. This was deemed sufficient to indicate a proper mix. At twenty-eight days four cylinders were removed and tested for compressive strength. The resulting average of 29,010 kPa was lower than the 44,120 kPa target value, but indicated that proper curing and strength gain was occurring. After these tests the base slabs were left to cure for an additional seven months. At the end of the eight-month period, another two beams and four cylinders were extracted for strength tests. The flexural beams reached an average of 4130 kPa and the compressive cylinders reached an average strength of 38,790 kPa. Both of these values were still slightly below the desired range, but close enough for other preparation work to begin.

### **5.3 PREPARING THE BASE BEAMS**

Between the casting of the base slabs and commencement of preparation work, nearly nine months passed. During this considerable time a proper review of relevant literature was undertaken. The specifics of how this research affected the proposed testing program will be discussed in Chapter 6. Aspects directly relevant to this chapter, however, include the size of member chosen for the fatigue testing program and methods of final preparation.

#### **5.3.1 Resizing and Cutting**

The element finally chosen for the testing program was a beam 0.406 m wide by 1.524 m in length. Instead of utilizing the 0.914 m wide by 1.829 m long slabs as they were cast, the narrower beam elements were cut from the slabs. The length was left the same because the excess could hang over the ends of the supports in the testing frame without causing interference. The width of the desired beam, however, was slightly less than half of the slab dimension. In order to maintain an even number and spacing of reinforcing bars, a 0.102-m-wide strip needed to be cut and removed from the middle of the slab. A professional concrete service was hired to cut the slab with a hydraulically driven saw-cutting machine. Figure 5.3 shows a stack of the base beam elements after saw cutting.

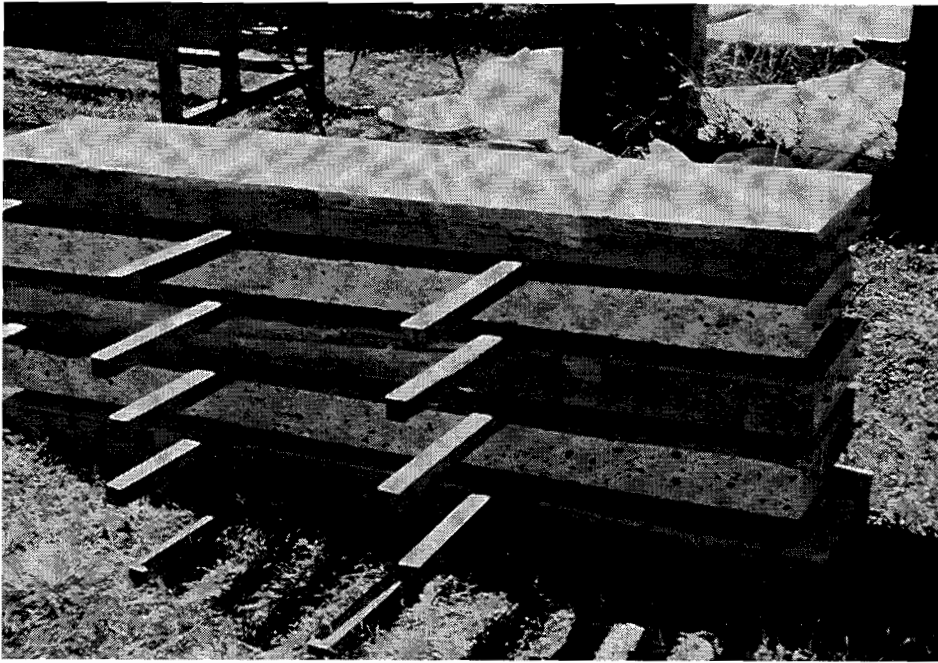


**Figure 5.3. Base Beams After Saw-cutting**

### **5.3.2 Cracking**

Although the El Paso pavement is considered to be in good condition overall, roadway surveys have been performed to precisely monitor the extent of cracking and general deterioration from thirty years of usage. The surveys revealed that several sections do exhibit signs of distress and modulus deterioration (Ref 1). Therefore, as a factor in properly simulating the pavement stiffness, cracking of the base beams was considered a necessary precursor to casting the overlay. This operation of strategically placing a full section crack at midspan also allows for more consistent behavior and results during actual fatigue testing. For purposes of testing uniformity, all the beams were pre-cracked at the same time even though some would not be overlaid for several months. To crack the beams fully through their cross-section, a two step process was performed.

The cracking process began with the placement of each base beam in a loading frame. The beams rested on simple supports at each end with a five foot spacing in between. A

hydraulic ram was lowered down so as to just rest on the beam at midspan. A steel plate distributed the ram's point load across the full width of the beam in order to ensure uniform cracking across the section. The loading proceeded at a uniform rate until a crack formed on the bottom face at midspan of the beam. The crack was allowed to propagate approximately half way up the section depth. At this point the load ram was raised and the loading was discontinued so as to not cause any damage to the beam.

After this first step, the beams were removed from the loading frame and flipped over so the uncracked face lay on the bottom. The beams were then put back into the frame and a loading process similar to the first step proceeded. Now when the bottom face cracked, the beams had a crack at midspan which ran the full width and depth of the member. Because of the two step process used, no other damage such as steel yielding or concrete crushing within the beams occurred. A close-up of the cracked section is shown in Figure 5.4

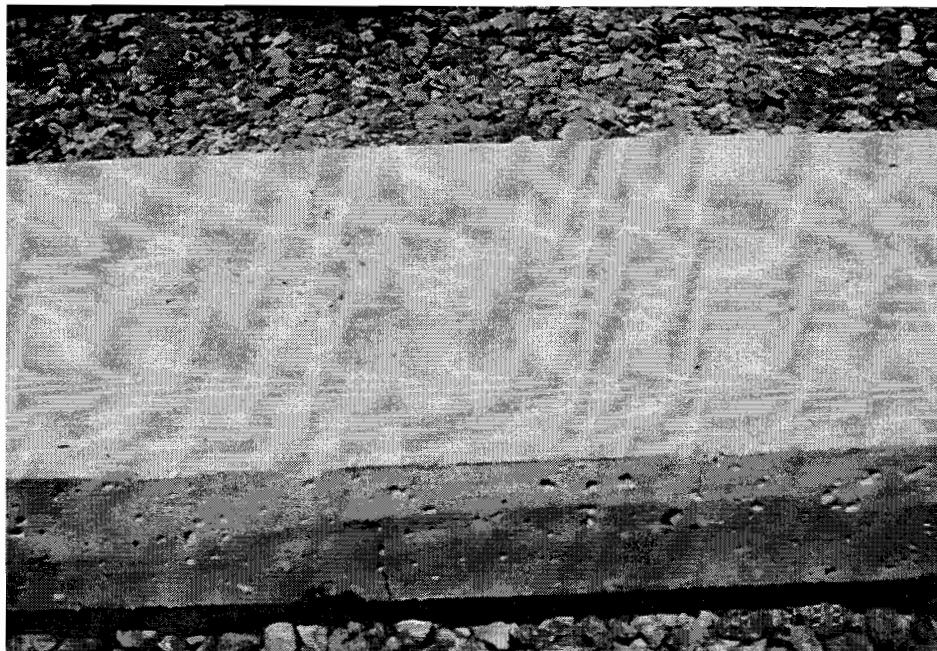


**Figure 5.4. Cracked Section of Base Beam**

### 5.3.3 Shotblasting

The final step in preparing the base beams before casting the overlay involved roughening the top surface. Bond development is a critical factor in the behavior of an overlay and developing positive interlock across a roughened surface increases the bond capacity of the overlay. Results from previous research indicate that effective methods of roughening a base surface include scarification, sandblasting, shotblasting, and hydrocleaning. For this project, with the limited size of the base members, only sandblasting and shot-blasting presented viable options. Since shotblasting has been tested as an effective method on previous large scale overlay projects (Ref 6) and will most likely be the method of choice for the actual El Paso overlay, it was picked as the most appropriate way to roughen the base beams.

For the shotblasting of small areas, manually operated versions of large-scale pavement machines are available. A Blastrac® 1-8D Unit MK4 model was chosen for use because of its small size, light weight, and ease of operation. This machine, pictured in Figure 5.5, has a working track 10.0 cm wide by 15.0 cm long. Several sizes of steel shot were available with this machine. After performing trial runs to determine the effectiveness of each shot size, an S460 shot was selected. This size of shot properly removed the surface paste and exposed the aggregate beneath without severely gouging the beams.

Shotblasting machines such as the Blastrac operate on a simple concept of forced air circulation and magnetism. Shot is placed into the machine through a grate at the top of the machine housing. When operating, air pressure propels shot from this reservoir down to an opening which sits directly on the pavement. The force of air pressure gives the shot sufficient energy to bombard the concrete surface and create the desired roughness. The air flow and subsequent rate of shotblasting can be controlled from a manual lever. After the shot has blasted the pavement, the magnetic base housing pulls it back up into the system for recirculation. The Blastrac is designed to operate most effectively with a vacuum attachment. The vacuum serves to pull the fine concrete dust from the return air stream and leave only the steel shot in the operating flow. This gives a cleaner and more uniform shotblasted surface.

To facilitate a consistent surface roughness among the beams, they were arranged together in a side-by-side fashion to create a platform area. With this larger working area the Blastrac was easily maneuvered across the beam surface in a regular back and forth fashion. Two to three light passes were typically required to achieve the desired roughness. This cautious approach was taken to ensure that the first pass did not excessively gouge the surface.

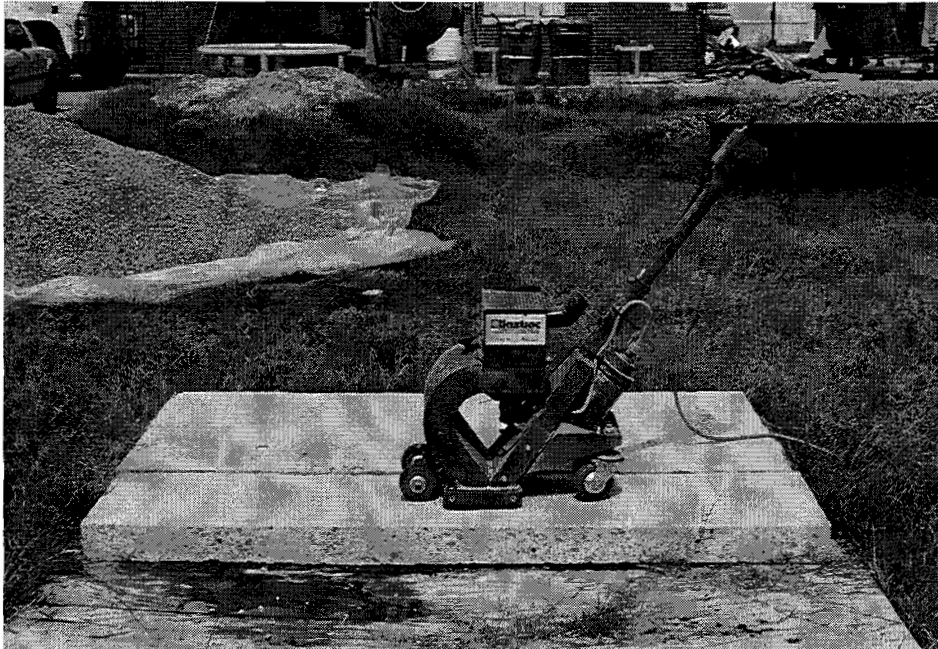


**Figure 5.5. Blastrac Shotblasting Machine**

The final product of this shot blasting operation was a base beam with a uniformly textured surface (Figure 5.6). The weak surface laitance had been removed and the aggregate fully exposed to create a proper interlock surface for bonding the overlay. No significant deviations in roughness between the twelve beams were noted. The texture closely resembled that produced for the previous bond tests which yielded more than adequate bond strengths. Figure 5.7 reveals a close

inspection of the roughened surface. When measured by the sand patch test (Ref 5), the beam surface had an average texture depth of 1.15 mm. This meets the minimum 1.14-mm roughness specified in a recent Louisiana project (Ref 20) but falls below the Houston requirements. Since these numbers are guideline recommendations and the surface appeared properly roughened, shotblasting was considered adequate.

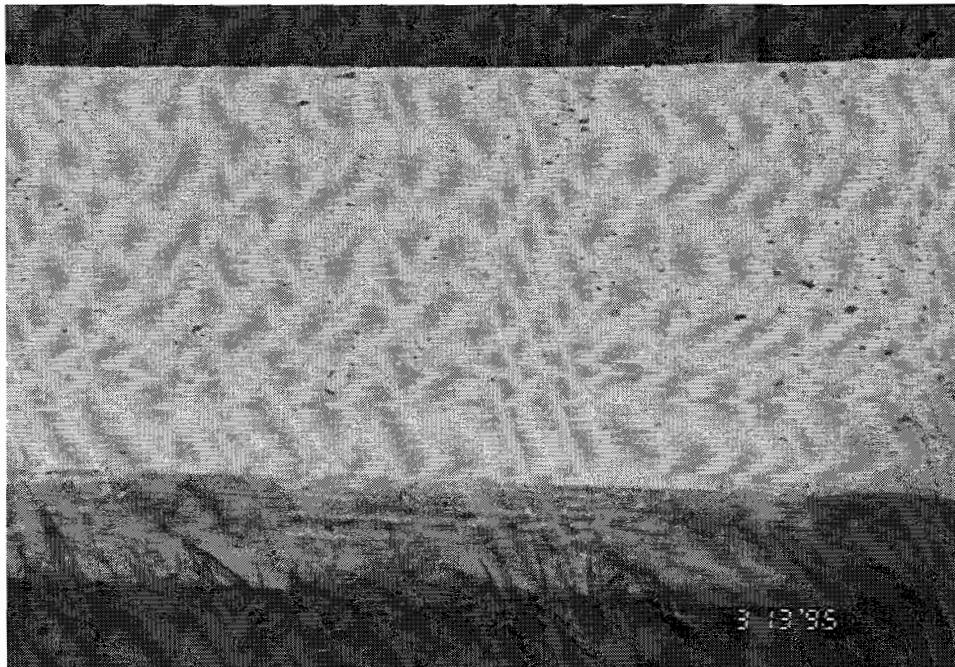


**Figure 5.6. Shotblasted Base Beam**

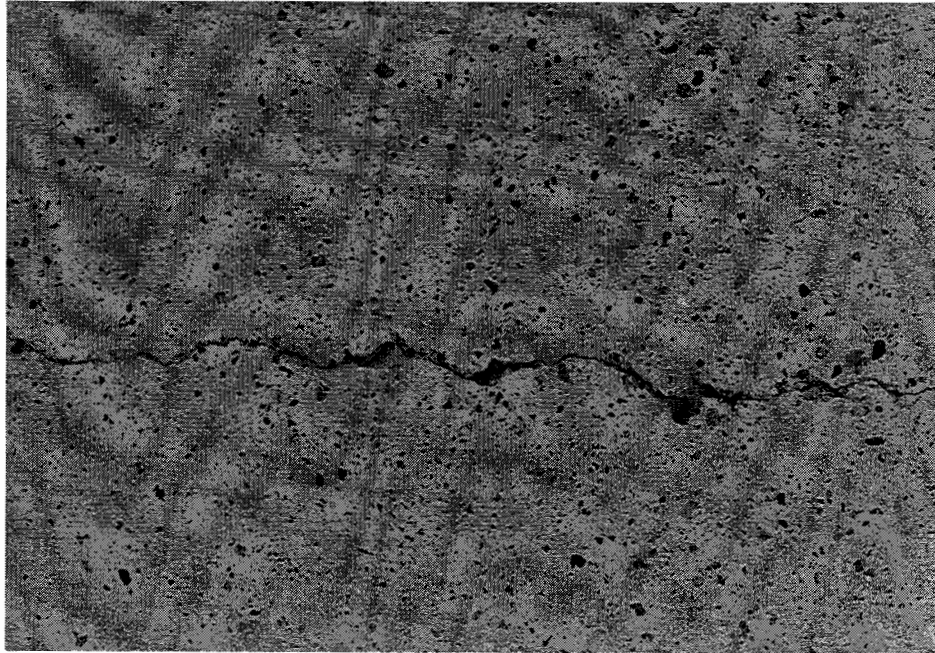


**Figure 5.7. Shotblasted Beam Surface**

#### **5.3.4 Debonding**

One base beam needed further preparation after shot blasting. In order to test the effect of a locally debonded zone within the bonded overlay, a central region the full beam width and only 15.24 cm in length was isolated with a border of duct tape and treated with a debonding agent. Within this zone, Dayton Spirit J6® was applied to the beam surface with a paint brush. J6 is a liquid curing and debonding compound most commonly used in lift-slab and tilt-wall construction. According to the manufacturer's directions, two coats were applied to ensure full debonding. After flooding the surface with water, a first heavy coat was applied. This coat soaked into the concrete surface to create an impermeable chemical barrier. The second coat, applied at a lower application rate, formed a physical surface layer which prevented the overlay concrete from chemically bonding to the concrete below.

## **5.4 CREATING THE OVERLAY**

As the actual fatigue test of each beam specimen approached, the overlay mix was cast upon the base beam. Due to the length of time involved with the fatigue testing procedure and the need for a specific range of curing time for the BCOs, each overlay was cast at an independent time instead of during a single operation. This actually simplified matters due to the large effort involved in hand casting only a single batch of the overlay mix.

### **5.4.1 Overlay Depth**

Studies were performed at Center For Transportation Research to determine the actual overlay thickness needed for IH-10 in El Paso. Although preliminary estimates based on previous experience centered around 7.62 cm, computer modeling soon proved this value far too low to achieve the desired thirty-year life span with suitable certainty. Factors such as the depth, stiffness and cracking of the original pavement were entered into two different computer programs for the purpose of predicting the necessary overlay depth. Both the AASHTO method and PRDS program were run using the data collected from road surveys and laboratory core testing (Ref 21). Several sets of data were entered in separate trials to account for stiffness variations between the sections of pavement surveyed along IH-10.

Thickness values produced by PRDS fell in the range of 9.14 to 14.22 cm while AASHTO values ranged from 13.97 to 25.40 cm (Ref 21). The discrepancy between the two solutions was due to the tighter confidence restrictions built into AASHTO. The thickness variance among each program's solutions arose from the variations in pavement section stiffness. Pavement designers at CTR decided to rely on the larger thickness values produced by the AASHTO method. For uniformity, the pavement section with the lowest stiffness and subsequent highest overlay thickness was ignored. The final overlay thickness chosen, 15.88 cm, then met or exceeded all other required section thicknesses. At the time the fatigue testing program began, however, the established value was a slightly lower 15.24 cm. Since testing began with this value, it was maintained throughout the program even though the actual design thickness was raised slightly at a later date. This discrepancy fell on the conservative side.

Because the fatigue program specimens were at half scale, the overlay cast upon the base beams measured 7.62 cm in thickness.

#### **5.4.2 Formwork**

A simple rectangular form consisting of 1.91-cm-thick lumber was constructed to contain the overlay mix during the casting operation. As Figure 5.8 shows, this formwork created a space the same dimensions as the base beams and was adjusted with shims to make the necessary depth of 7.62 cm for the overlay. The formwork fit snugly to the base beam and movement was prevented with several bar clamps. After casting, the forms were easily removed by loosening the end screws and lifting the wooden frame directly upwards. In this manner the same form was able to be re-used for the casting operations. The smooth top edge of the wooden form also served as a screeding guideline to finish the overlay's top surface.

#### **5.4.3 Casting**

Application of the overlay concrete mix to the base beams followed a simple procedure which changed only slightly between specimens. When weather permitted, the base beam was placed outdoors for casting and curing. During rain-out periods, the process proceeded indoors until better conditions allowed the whole specimen to be moved outside. The overlay concrete mix was weighed and batched manually as previously described in Chapter 3. The concrete was shoveled into the beam form and consolidated with a needle-nose vibrator. After striking off the excess concrete with a wooden plank, a metal float was used to create a level top surface. A sufficient volume of concrete was batched to provide for at least twelve cylinder specimens. A finished beam, cast and cured outdoors, is shown in Figure 5.9.

#### **5.4.4 Curing**

As mentioned above, curing of the overlay proceeded outdoors if the weather permitted. The entire beam with overlay was layered in wet burlap and covered with clear plastic to ensure good hydration. This continued until cylinder tests revealed that the desired compressive strength had been reached for commencement of fatigue testing. For the beams cured to full strength before testing, no further curing was needed. Since the fatigue testing of most beams began at an early age and strength, however, continued hydration during the fatigue testing

program was necessary. For these specimens, the wet burlap and plastic were reapplied after the beam was moved into the testing frame.

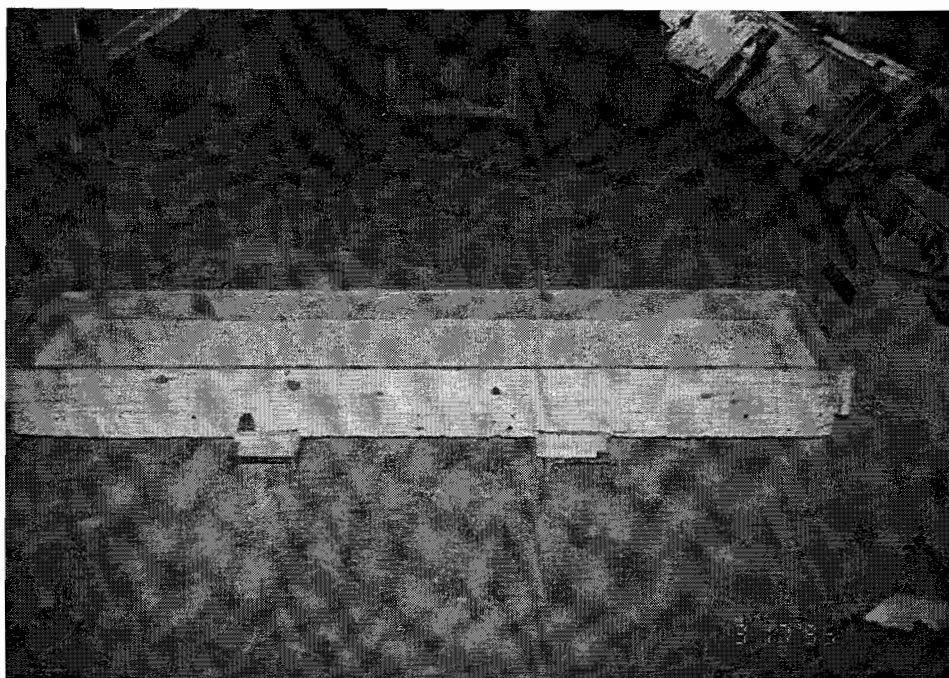


**Figure 5.8. Formwork For Casting Overlay**

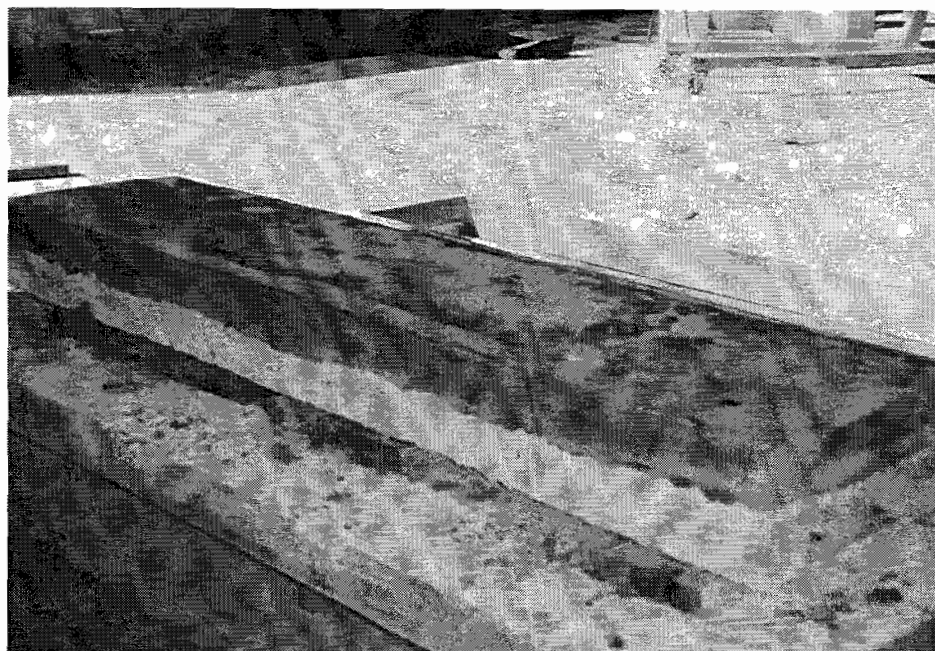


**Figure 5.9. Completed Bonded Overlay Beam Specimen**

## **CHAPTER SIX: FATIGUE TESTING PROGRAM**

The following chapter outlines the specific method of testing and equipment utilized for the determining the effects of early traffic loading on a bonded concrete overlay. A brief synopsis and defense of the testing method were given in Chapter 4.

### **6.1 TESTING EQUIPMENT AND GENERAL SETUP**

Fatigue testing of the bonded concrete overlay beams was performed at the Pickle Research Campus at The University of Texas in Austin. All equipment was located at the Construction Materials Research Building. Specific program parameters were geared towards working within the confines of the fatigue testing frame available at this location.

#### **6.1.1 Testing Frame**

The structural testing frame available for use at CMRG is wholly self-contained and does not rely on a reaction floor. The frame consists of a heavy open box structure formed by grade A36 steel wide flange members. The base of the box consists of two pairs of W21x68 beams. In the long direction of the frame, these beams permanently bolt to W12x50 columns. To provide adjustable support locations, the second pair of base beams bolt directly to the long beams instead of the columns. A grid of machined holes at a 75-mm spacing along the flange of the long beams allows the shorter support beams to be repositioned nearly anywhere along the length of the frame. The upper portion of the box, which supports the loading head, is formed from permanent W21x68 beams.

While the total interior dimensions of the frame box measure 2.13 m long by 0.71 m wide by 1.73 m in height, only a portion of this volume is actually available for testing. The suspended loading head extends downwards a minimum of 1.22 m. This leaves 0.51 m of specimen height available for direct use. Also, roughly five cm of clearance space must be maintained from the end columns. Figure 6.1 shows an overall view of the testing frame from the direction of the testing room access door.

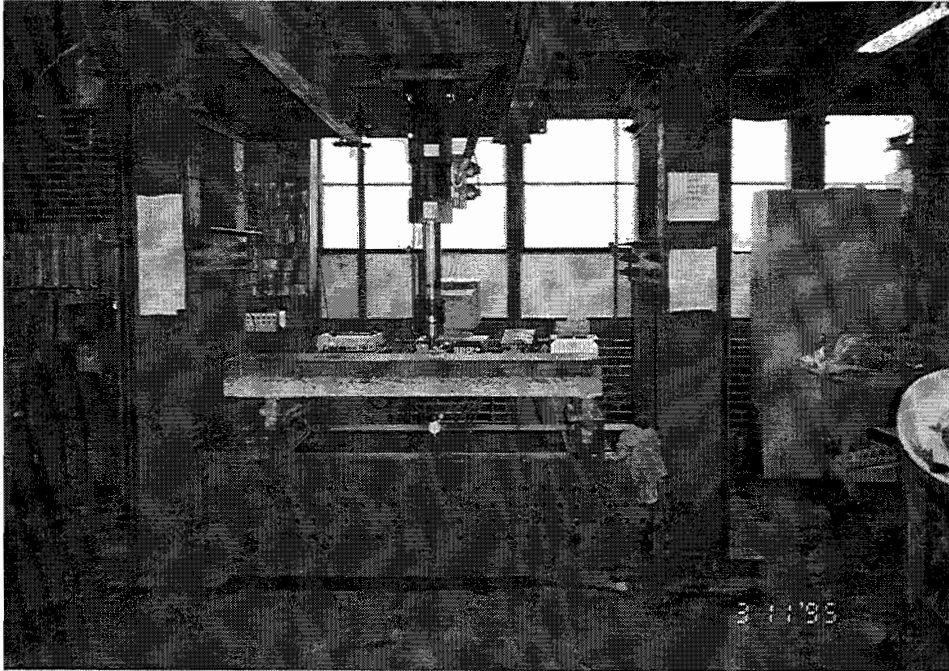


**Figure 6.1. Fatigue Testing Frame**

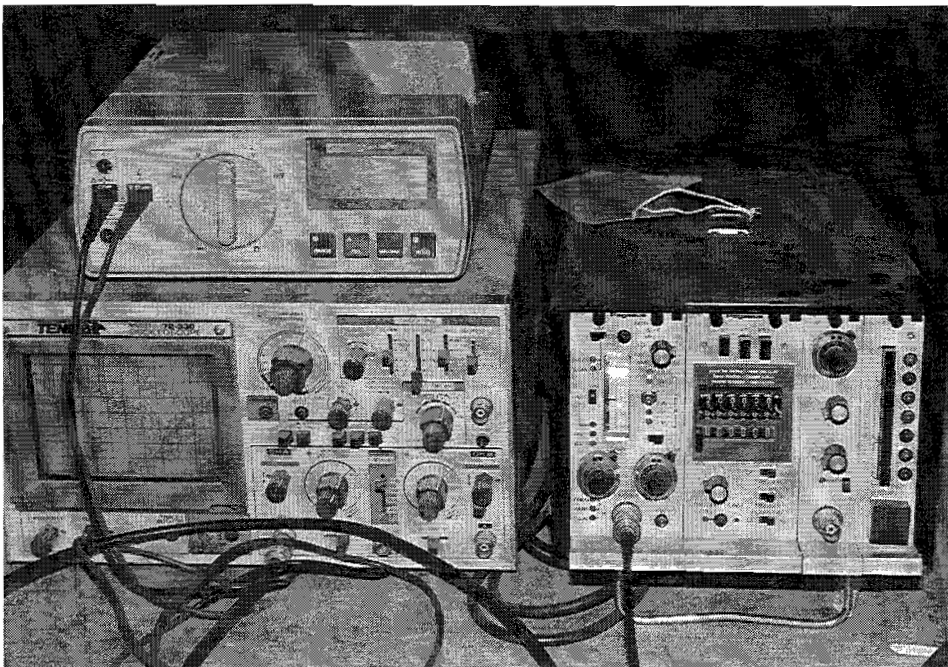


**Figure 6.2. Pegasus Load Controller and Support Equipment**

### 6.1.2 Load Cycling Apparatus

The ram suspended from the frame's upper box is a Materials and Tests (MTS) loading head with a 250 kN fatigue rated capacity and a 15.0 cm travel range. For considerations of noise and vibration, the Wilson hydraulic pump is contained in a separate housing behind the CMRG laboratory. Operation of the loading head is achieved with a Schenck Pegasus 5100 series servo-controller (Figure 6.2) through a feed back circuit. Control units within the Pegasus can adjust all major functions including loading rate, static load, cyclic load range, cyclic frequency type, and cyclic frequency rate. The Pegasus was fully serviced and calibrated before being used in the fatigue program.

By replacing an internal bridge resistor and calibrating a series of external voltage controls, the Pegasus load controller can be adjusted to operate at any desired maximum voltage and load output. The internal bridge resistor was replaced with a 151  $\Omega$  chip and adjustments made to set the maximum load at the MTS's rated capacity of 244,640 N. The maximum output voltage was set at 10.00 volts by placing the excitation voltage at 7.55 volts. These adjustments were performed using the following equation:

$$V_o = R * XDCR * V_{exc} * G \quad \text{Eq. 6-1}$$

where  $V_o$  = Output voltage

R = Ratio of load setting to load capability

XDCR = calibrated sensitivity of 0.002

$V_{exc}$  = Excitation voltage

G = Gain ratio of 100,000/151

The static and span load control dials on the Pegasus have a ten-turn capacity with fifty markings per turn. A full ten turns corresponds to the maximum load setting of 244,640 N. Static loads are set by a direct ratio of turns on the static load dial. Cyclic load ranges are set with a combination of both dials. The static load dial is first set at the median value within the desired range. The span load dial is then set to the value of fluctuation above and below the

median value. This additive and subtractive loading arrangement yields the full range of desired cyclic loading. The rate of cycling is also controlled by a ten turn dial.

### 6.1.3 Beam Strength And Load Calculations

To determine a proper loading range for fatigue testing, calculation of the composite beam's flexural strength was required. The maximum load during fatigue cycling is commonly set at fifty to sixty percent of member capacity as a first trial. A calculation of the overlay interface shear caused by this load was also necessary. Optimally, the interface shear created at the maximum of the load cycle would approach 207 kPa. Previous studies have determined this to be the value of interface shear caused by traffic loading on a bonded concrete overlay pavement (Ref 11).

The flexural yield capacity of the composite beam was determined using strain compatibility at yield. This calculation required knowledge of the beam's material properties and sectional dimensions. Steel properties were verified through coupon testing and the concrete modulus assumed a fully cured overlay compressive strength of 51,700 kPa. The three #3 reinforcing bars (9.5 mm) in each beam accounted for a total steel area of 0.838 cm<sup>2</sup>. Depth to steel averaged 13.97 cm and cross-section width measured 40.64 cm. Samples of the grade 60 ksi rebar tested at a yield strength of 437,140 kPa (63.4 ksi) and a yield strain of 0.0022 cm/cm. Modulus of elasticity for the full cured overlay was 37.58 MPa.

In Eq 6-2 the tension and compressive forces acting on the cross-section were equated. By solving the quadratic for the unknown term "c", a value of 2.54 cm was obtained for the depth of compressive stress block. The flexural yield capacity of 12,250 N-m was then calculated in Eq 6-3 by summing moments of forces about the reinforcing steel depth.

$$A_s F_y = \frac{b * c^2 * \epsilon_y * E_c}{2 * (d - c)} \quad \text{Eq 6-2}$$

where  $A_s$  = cross-sectional area of reinforcing steel

$F_y$  = reinforcing steel yield strength

$\epsilon_y$  = reinforcing steel yield strain

$E_c$  = concrete modulus of elasticity

$d$  = total depth to reinforcing steel

$b$  = cross-sectional width

$c$  = compressive stress depth

$$M_y = A_s * F_y * (d - c / 3) \quad \text{Eq. 6-3}$$

where  $M_y$  = composite beam flexural yield capacity

At sixty percent of this yield capacity the maximum applied moment would be 7,345 N-m. The moment consisted of both the applied single point load and the beam's inherent dead weight. Over the five-foot unsupported length, the beam weight resulted in a midspan moment of 497 N-m. The remaining 6848 N-m corresponded to a point load of 18,245 N. Although the moment calculations would vary slightly with a small loading plate instead of a point load, this value was chosen as the initial maximum cyclic load.

The interface shear stress was computed from the combined loading effect of the beam weight and maximum fatigue load over the unsupported five foot span. Interface shear is calculated using the following state of stress equation:

$$T = \frac{VQ}{Ib} \quad \text{Eq. 6-4}$$

where  $V$  = shear stress due to applied loads

$Q$  = moment of overlay area about centroid

$I$  = section moment of inertia

$b$  = cross-sectional width

The maximum applied shear under the fatigue load and dead weight would be 10,408 N. Using a modular ratio of 5.3 for steel area transformation, the cross-sectional moment of inertia was 19,108 cm<sup>4</sup>. With an overlay moment area of 1,311 cm<sup>3</sup>, the total interface shear stress

produced would be 176 kPa. This value of interface stress fell slightly below the target of 207 kPa, but not sufficiently low to merit an increase by means of increasing the beam span or applied load.

#### 6.1.4 Testing Setup

Fatigue testing of the beam specimens was performed on a simply-supported basis. The testing frame's support beams were moved to an even spacing on either side of the loading ram with a total separation of 1.524 m. The simple supports consisted of a greased steel roller at one end and a stationary roller at the other. Each measured 45.7 cm in length and fully supported the entire width of the beam. Both supports were welded to steel plates for stiffness and added weight to prevent movement. Due to the loading head's limited range of movement, additional spacing elements were required to elevate the beam within the head's travel path. These spacers consisted of welded steel channel elements reinforced at top and bottom with steel plates. Figure 6.3 is an end view of the total support.

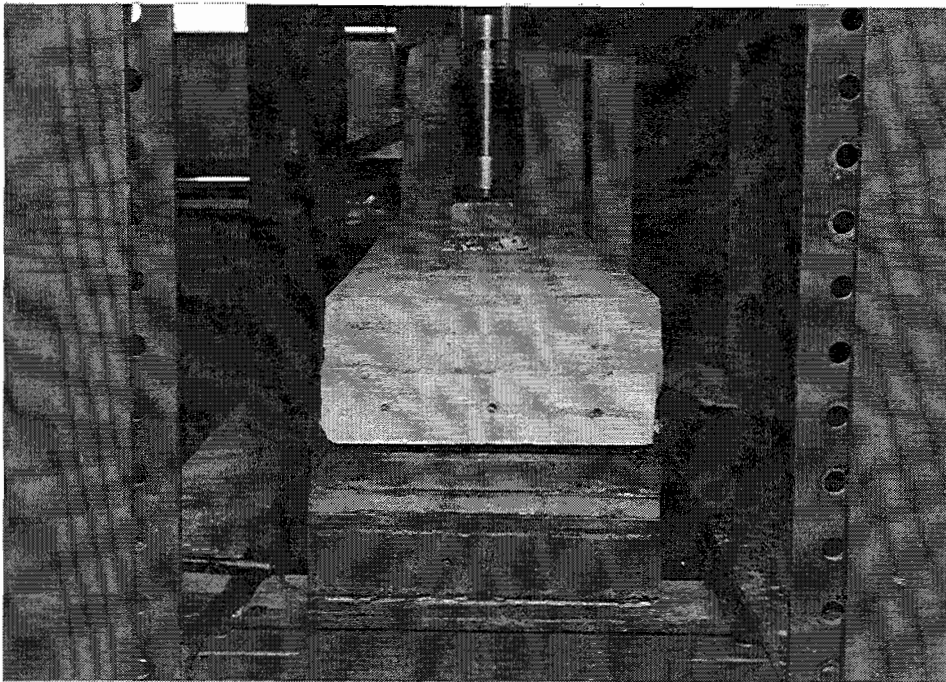


**Figure 6.3. End Support With Spacing Element**

To simulate the tire pressure of an eighteen-wheel truck during loading, the point load of the overhead ram required distribution by a stiff steel plate. A 2.54-cm-thick plate was used. By adjusting the area of this plate, the loading pressure applied to the beam surface would vary. An initial estimate of maximum load for the fatigue program was 18.25 kN. To achieve a standard 620.5 kPa (90 psi) pressure, the plate required an area of 286.7 cm<sup>2</sup>. The actual plate used measured 15.24 cm to a side, or an area of 232.3 cm<sup>2</sup>. This smaller size yielded a slightly larger pressure of approximately 758.3 kPa (110 psi). The smaller size was chosen due to restrictions in space on the surface of the beam.

As mentioned in Chapter 5, the beam specimens were left at their original 1.829-m length even though only a 1.524-m clear span would be used during testing. The line of the base beam pre-crack lay directly centered along the full beam length. The loading plate needed to be offset to the side of this crack location to properly simulate tire travel along a pavement. Also, placing the steel plate above the crack would have created an artificially stiff region at the point of highest stress.

Before placing the beam into the testing frame, two steel bearing plates were affixed to the beam's bottom face over the support locations. These plates, attached with hydrostone, served to distribute the support load evenly and prevent concrete crushing at early ages. The top loading plate was also secured into place with hydrostone. The base plates were attached at a 0.76-m spacing away from the loading plate's center point such that the load plate lay directly between support locations. Figure 6.4. shows the attached loading plate and an additional steel spacing block.

For the purpose of monitoring beam deflections during the testing program, a dial gauge was placed on a stand directly beneath the base beam pre-crack location. The Fowler gauge has a travel range of 1.27 cm and an accuracy of  $2.54 \times 10^{-4}$  cm. The gauge was clamped to a steel rod which screwed into a heavy, stable base plate. During actual load cycling the gauge rod was retracted and restrained with duct tape to prevent possible damage to internal mechanisms. To take a static load deflection reading the tape was removed and the rod allowed to spring back into

place. In Figure 6.5 the gauge sits beneath the beam. Figure 6.6 pictures the beam prior to testing.

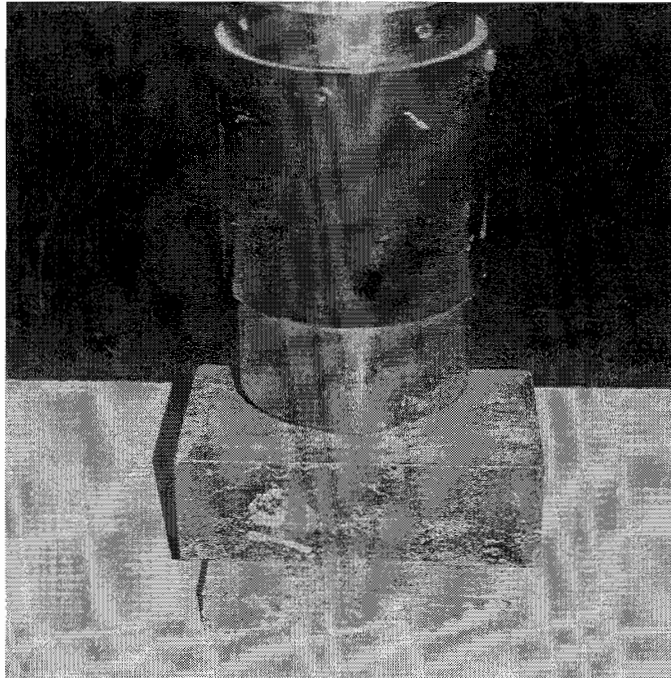


**Figure 6.4. Loading Plate and Spacing Block**

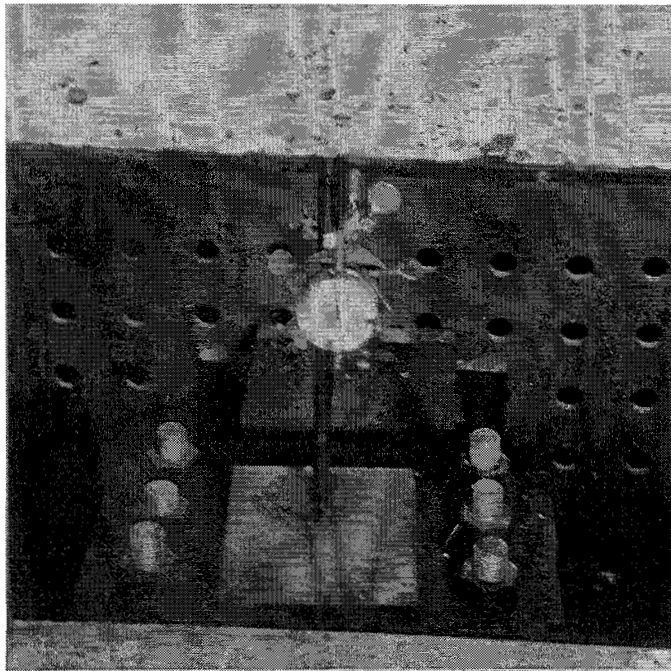


**Figure 6.5. Deflection Dial Gauge Beneath Beam**

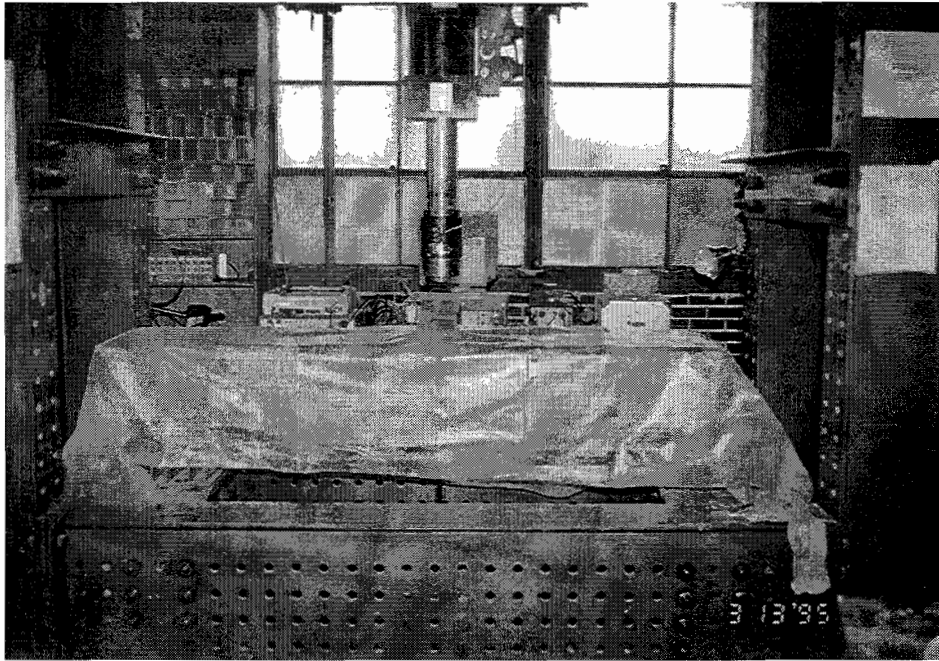


**Figure 6.6. Beam Prior To Testing Commencement**

### **6.1.5 Additional Equipment**

Because the Pegasus is an older model without digital display readings, a few items of support were necessary to ensure proper loading and fatigue cycling. A digital multimeter was plugged into an output jack of the Pegasus. Readings of the present, previous minimum, and previous maximum voltage output were obtained from the multimeter display. From these voltage readings a direct conversion to load was achieved through a simple formula. The ratio of present voltage to maximum output voltage is equivalent to the ratio of present load to maximum load setting. Thus the current load could be obtained through multiplying the rated capacity of 244,640 N by the ratio of present to maximum voltage.

$$\text{Load} = \frac{\text{Voltage}}{10.00} * 244,640 \qquad \text{Eq. 6-6}$$

This calculated load could then be compared with the value expected from control panel settings. A match indicated proper operation.

To visually verify the cyclic loading wave form, an oscilloscope was also connected to the Pegasus. The oscilloscope is pictured in Figure 6.2. By comparing the range of the cyclic wave on the monitor with voltage settings on control dials, the magnitude and range of the load was visually verified. The oscilloscope also allowed verification that the loading consisted of the desired sine wave pattern.

## **6.2 TESTING PROCEDURES**

This section fully defines the exact process used during the testing of each overlay beam specimen. This includes tests performed during the actual fatigue program and additional testing done afterwards. The same process was followed for all beams.

### **6.2.1 Preliminary Operations**

The first beam specimen placed into the load testing frame was one of two with fully cured overlays. After properly aligning the beam and adjusting the spacing supports, the Pegasus load controller was turned on and the loading head lowered into contact with the top spacing block. The dial gauge apparatus was positioned beneath the beam and the unloaded gauge reading recorded. The specimen was now ready for testing to begin.

Before beginning the cyclic loading, a static deflection reading was taken. By adjusting the Pegasus static load dial to seventy-five units of one turn, a static load of 18,245 N was gradually applied. This static load corresponds to the maximum load application during cyclic testing. A reading of the dial gauge deflection was subsequently recorded. While in the loaded position, measurements of crack locations and lengths were taken. A scaled drawing showing crack locations was compiled. After removing the static load, the reading was again recorded to measure the new unloaded deflection. At this time the dial gauge rod was retracted and secured with duct tape.

### **6.2.2 Operations During Fatigue Testing**

The Pegasus control panel was now set for cyclic loading. The static dial was set to forty-one units of a turn which corresponds to a median load of 10,013 N. The span dial was set

to thirty-four units of one turn, corresponding to a span load fluctuation of 8,233 N. Thus the total range of cyclic loading progressed from 1,780 N to 18,245 N. The low end of the cyclic load path was not set to zero because a minimum load amount was necessary to prevent the ram head from losing contact with the specimen. A minimum load of ten percent of the maximum is generally considered acceptable.

After lowering the ram head into position with the static load value, the load cycling process began by activating the necessary control switches. The frequency of cycling was adjusted manually to three cycles per second. Beyond this rate the ram head tended to chatter against the loading plate. The chatter was caused by the beam's relatively low stiffness and inability to cyclically deflect as quickly as the load ram.

At each 250,000 cycle interval, the load cycling process was temporarily halted to take a static load deflection reading and map further beam cracking. Both these processes proceeded exactly as described for the preliminary operations. At a rate of three Hz each interval took approximately twenty-three hours to complete. In order to remain on a twenty-four hour testing cycle, this allowed one hour for performing the static load test and crack mapping. During this time the burlap mats covering the beams were resoaked to provide optimal continued hydration. The fatigue process continued for a total of 2,000,000 load cycles.

The parameter chosen to define the failure of a beam during fatigue testing was the net increase in static beam deflections after 2,000,000 cycles. A one hundred percent increase in the fully loaded static deflection from the initial pre-cyclic reading to the final reading at 2,000,000 cycles would constitute a successful fatigue test. Beam #1, with a fully cured overlay, was used as the baseline reference. Significant deviation from this criteria would require adjusting the fatigue load range chosen from preliminary calculations. Because the deflection increase for beam #1 closely matched the chosen criteria, however, it was not necessary to adjust the loading range for subsequent beam tests.

### **6.2.3 Schedule of Testing**

In order to determine the effects of traffic loading at early ages, the bonded overlay beam specimens were tested at a variety of ages and strengths. By observing the response of these

members to fatigue loading at sequentially lower overlay ages, an overall picture of the early traffic loading effects could be collected for later evaluation.

To establish a solid reference point of behavior for the early age members, a pair of fully cured beams were first tested. These beams served as a guideline from which all other testing measurements were compared. For the purposes of this experiment, a fully cured overlay was defined as a compressive strength of at least 48,260 kPa . This was the lowest value reached at twenty-eight days in the previous mix testing program. Subsequent beam tests began at earlier ages of overlay curing. Because weather conditions tended to vary during the curing of each beam, actual age of the overlay tended not to be a reliable indicator of capacity. Thus, instead of beginning each beam fatigue test at a specific age, a value range of overlay compressive strength was dictated. In this manner a reliable progression of relatively less stiff members could be achieved.

Table 6.1 outlines the original sequence of beam testing and desired compressive strength range (kPa) at the beginning of fatigue testing. It should be noted that this original schedule was revised during testing as results revealed a behavior less susceptible to early age fatigue than expected. After beam four, the program was changed to include several beams at substantially lower initial compressive strengths. Furthermore, the two stage loading was eliminated completely. The concept of a two stage fatigue process arose from the expectation that at low early strengths the beam specimens would be severely damaged by rapid cyclic loads. Since the cyclic rate of three Hz produces loads at a substantially faster rate than any traffic conditions, it was considered more realistic to apply a slower rate to beams five and six until more complete curing occurred. Table 6.2 shows the revised schedule of beam testing with the additional low strength beams and eliminated low-cycle program.

#### **6.2.4 Operations After Fatigue Testing**

After the completion of the 2,000,000 load cycles, each beam was tested under additional static load to verify the design strength. The load was applied until substantial cracking, deflection, and yielding occurred within the beam. At intervals during the load process

deflection readings were recorded and cracking mapped. Upon completion of a load testing the bearing plates were removed and the beams were stored behind the laboratory building.

**Table 6.1. Original Schedule of Beam Testing**

<b>Beam Number</b>	<b>Overlay Compressive Strength Range at Low Cycle Fatigue Initiation (kPa)</b>	<b>Overlay Compressive Strength Range at Full Cycle Fatigue Initiation (kPa)</b>
1	not applicable	fully cured = 48,260
2	not applicable	fully cured = 48,260
3	not applicable	27,570-31,020
4	not applicable	27,570-31,020
5	18,960-22,400	27,570-31,020
6	18,960-22,400	27,570-31,020

**Table 6.2. Revised Schedule of Beam Testing**

<b>Beam Number</b>	<b>Minimum Overlay Compressive Strength at Fatigue Initiation (kPa)</b>	<b>Maximum Overlay Compressive Strength at Fatigue Initiation (kPa)</b>
1	fully cured = 48, 260	-
2	fully cured = 48, 260	-
3	27,570	31,020
4	27,570	31,020
5	18,960	22,400
6	12,060	15,510
7	12,060	15,510

### 6.2.5 Additional Tests

During the eight-day progress of the fatigue testing for each beam, compressive cylinders were periodically tested. These cylinders from the overlay mix batching had been cured under wet burlap and plastic beside the testing frame. The similar curing conditions were done in order to yield the closest possible evaluation of compressive strength development in the overlay.

At the conclusion of fatigue testing all seven beam specimens were cored for the purpose of conducting a bond shear test of the overlay interface. Using a 10.16-cm diameter drill barrel, one full-depth core sample was taken from each end of every beam. Care was taken to avoid cutting through reinforcing steel, as this might have caused undue stress on the interface while drilling. These seven core samples were subsequently tested for bond shear strength in the guillotine apparatus described in bond testing section of Chapter 3. At the opposite beam end an additional core was drilled to a depth of 8.89 cm, cutting through the overlay and partially into the base. These cores were tested in-situ for direct tension bond capacity. For this test a steel plate was bonded to the overlay surface and pulled up in tension with a rotary screw device (Ref 6). Both methods were used to determine if proper bond had been achieved from shotblasting and whether fatigue testing had deteriorated the bonded interface. Figure 6.7 shows the beam #1 full-depth core sample after guillotine testing. In Figure 6.8, a direct tension pull-off core from beam #5 fractured in the base slab at 1.25 cm below the interface. The darker top layer is the overlay mix concrete.

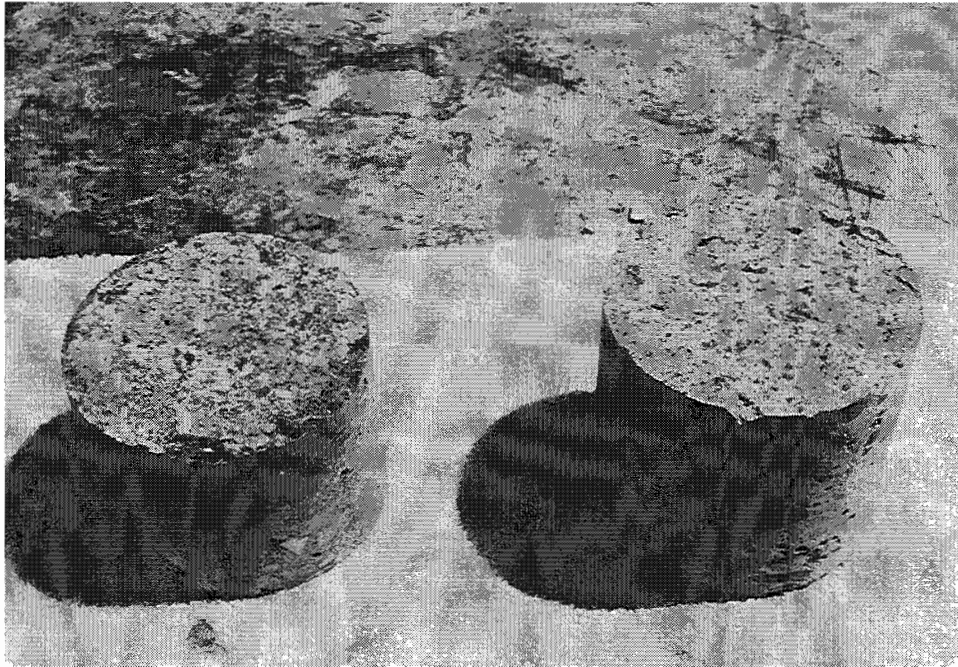


**Figure 6.7. Full-Depth Core Sample of Fatigue Beam**

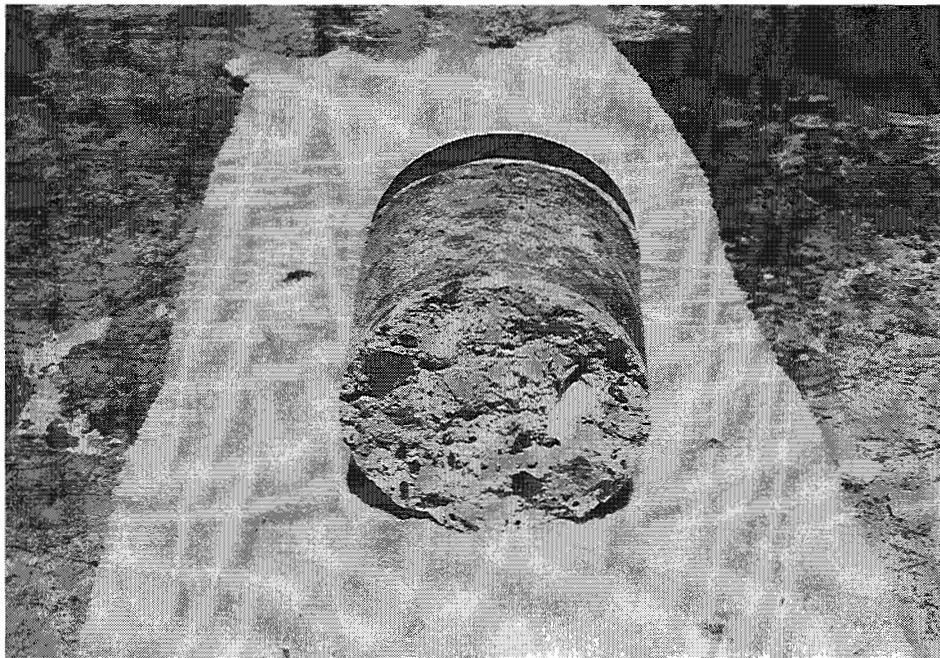


**Figure 6.8. Direct Tension Core Sample of Fatigue Beam**



## CHAPTER SEVEN: RESULTS OF FATIGUE PROGRAM

Results from the fatigue loading program fall into three categories. The first includes data from static load deflections and crack mapping of the fatigue beam specimens. This information must be directly correlated with the compressive strength gain of the overlays during the eight-day fatigue testing operation. Lastly, testing of cored beam samples yields information on the interface bond strength.

### 7.1 STATIC LOAD DEFLECTIONS AND BEAM CRACKING

At each 250,000 cycles during the fatigue loading of the beams, a deflection reading was taken under the full 18,245 N static load. Cracks along the beam side were also measured and sketched. Beam #1, one of two beams with a fully cured overlay, was the first beam tested. It also served as the control for whether to maintain the calculated loading range the same for further tests. Since the deflections for beam #1 closely followed the criteria set forth in Chapter 5, undergoing nearly a one hundred percent increase in static load deflections after 2,000,000 cycles, the first test was considered successful, and the loading range was not altered.

#### 7.1.1 Static Load Deflections

Figures 7.1 through 7.7 chart the results for the static load deflection readings of beams one through seven. The measurements taken after each 250,000 cycles included an unloaded deflection, a deflection at full static load, and a return unloaded deflection. All deflection data may be found in Appendix A and are partially summarized in Table 7.1. The change in unloaded deflection readings at zero cycles (before fatigue loading began) resulted from the cracking which occurred during the first application of full static load. At all other times the return deflection readings were taken only to verify the initial unloaded reading and any slight variations between the two were exclusively due to minor fluctuations in the load voltage.

The fatigue testing of beam #1 began after the overlay reached a fully cured compressive strength of 54,677 kPa. An initial static load deflection of 0.1074 cm was recorded. After 250,000 cycles this deflection increased by fifty percent to 0.1600 cm. This trend of increasing deflections continued with a progressively slowing rate until testing concluded. As Figure 7.1

shows, the deflections increased only a minimal 0.004 cm between 1,500,000 and 2,000,000 cycles. The increase in static load deflections during testing of beam #1 followed a nearly identical path of increase in the unloaded deflections. The relative deflection value, measured as the range from the unloaded to fully loaded reading, varied only from 0.1074 to 0.1095 cm. These minor variations, which followed no discernible trend, most likely arose from an inability to achieve the exact 18,245 N load application at each test cycle.

Fatigue beam #2, also fully cured to 48,955 kPa, produced a trend in results very similar to beam #1. The initial loaded deflection of 0.0973 cm progressively increased to 0.1824 cm at the conclusion of testing. Except for an unusual jump of 0.0115 cm between 1,750,000 and 2,000,000 cycles, a majority of the increases occurred early in testing. Again, the range of relative deflections varied only slightly from 0.0963 to 0.0980 cm. The strong correlation in results between the two beams with fully cured overlays verified that nothing unexpected had occurred during testing of either member.

Fatigue beams #3 and #4 underwent loading after reaching respective overlay compressive strengths of 30,614 kPa and 31,855 kPa. Beam #3 followed a deflection trend comparable with the fully cured specimens. The initial loaded deflection reading of 0.1113 cm increased by forty percent after 250,000 cycles. At 2,000,000 cycles the deflection had increased by seventy-eight percent to a final value of 0.1981 cm. The range of relative deflections did follow a definite trend. As testing progressed the relative deflection values steadily decreased from 0.0953 to 0.0922 cm. Fatigue beam #4, the companion to #3, was the first beam to deviate from this strong trend of increasing deflections. After 250,000 cycles the loaded deflection increased to 0.1412 cm, only twenty-one percent above the original 0.1184 cm. During the remaining 1,750,000 cycles, loaded deflections increased by only another 0.0173 cm to the final value of 0.1585 cm. Not only did the trend of increasing deflections flatten out much sooner than the previous three beams, but the final value fell a full twenty percent below that of its companion beam.

Load cycling of beam #5 began when the overlay reached a compressive strength of 20,892 kPa. Here, the previous trend of increasing deflections completely halted. During the

first 250,000 cycles, loaded deflections increased thirty-eight percent from 0.1240 cm to 0.1717 cm. An additional increase of only 0.0069 cm was measured in the remaining 1,750,000 cycles. As Figure 7.5 shows, the loaded deflection line remained essentially unchanged after the first 250,000 cycles. The unloaded deflections did continue to increase slightly during testing. The range of relative deflection values steadily decreased from 0.1057 to 0.0980 cm.

Beams #6 and #7 were cured to an overlay compressive strength of 13,514 kPa and 13,997 kPa. Beam #7, the last in the testing series, also had a central section of the overlay deliberately debonded from the base beam. In terms of trendlines, this pair of beams behaved exactly as beam #5. Specifically, however, all deflections were larger. The initial fully loaded reading for beam #6 measured 0.2146 cm. This increased by 0.0381 cm, or eighteen percent, to reach 0.2527 cm after 250,000 cycles. Virtually no change occurred after this point and the final deflection measured 0.2578 cm. The range of relative deflections, which began at 0.1171 cm and ended at 0.1077 cm, was slightly higher than for previous beams. Beam #7 had nearly identical loaded deflection readings. Beginning at 0.2141 cm, they increased to 0.2560 cm after 250,000 cycles, and concluded at 0.2586 cm. The relative deflections for beam #7 were the largest measured and changed the most during testing. They started at 0.1384 cm and gradually reduced to 0.1219 cm during testing.

At the conclusion of testing, all beams were examined for delaminations which might have affected deflection results. Except for the intentionally debonded region of beam seven, which did not spread, none were noted.

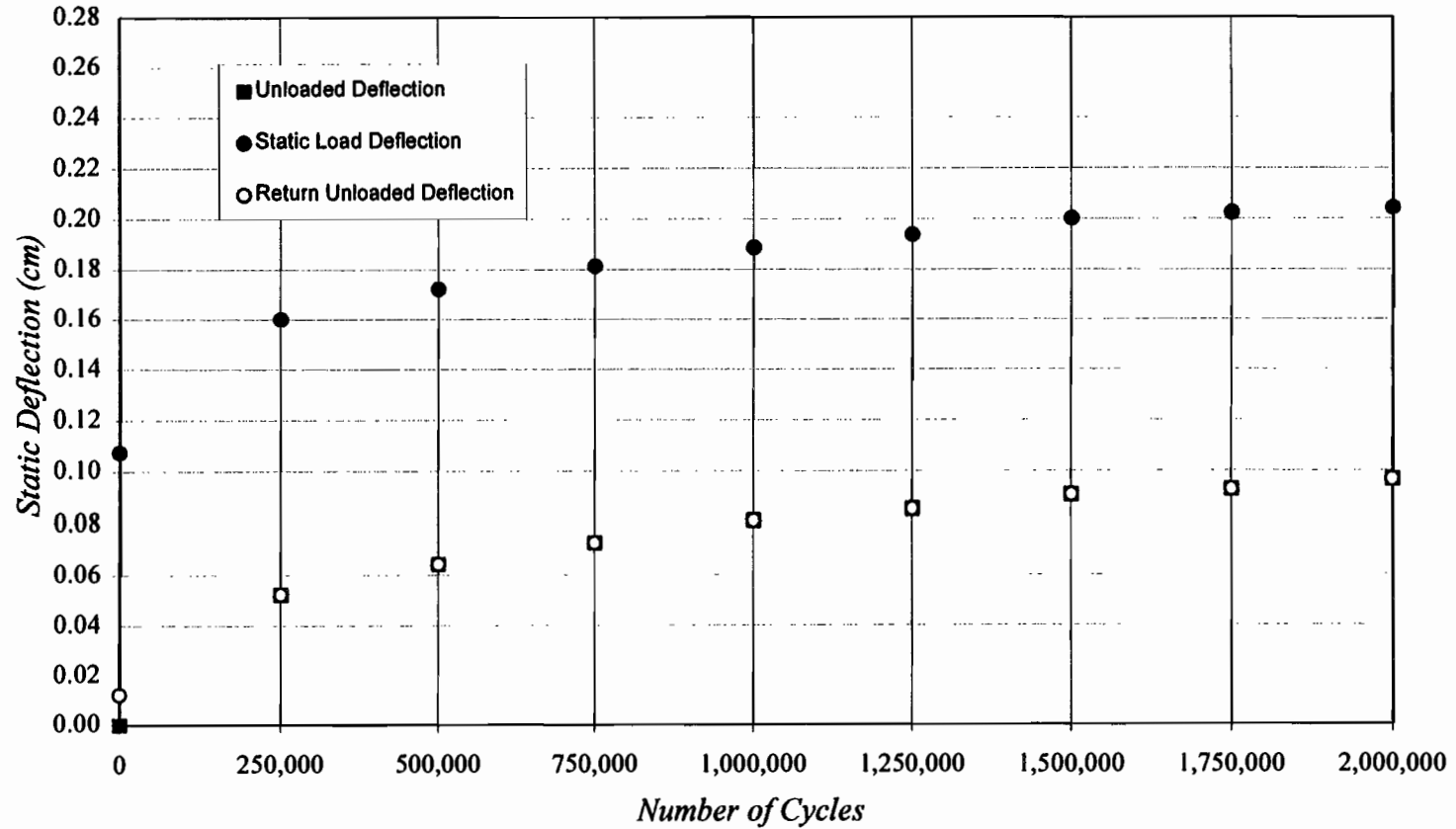


**Figure 7.1. Static Load Deflections For Fatigue Beam #1**  
**Initial Overlay Compressive Strength = 54,677 kPa**

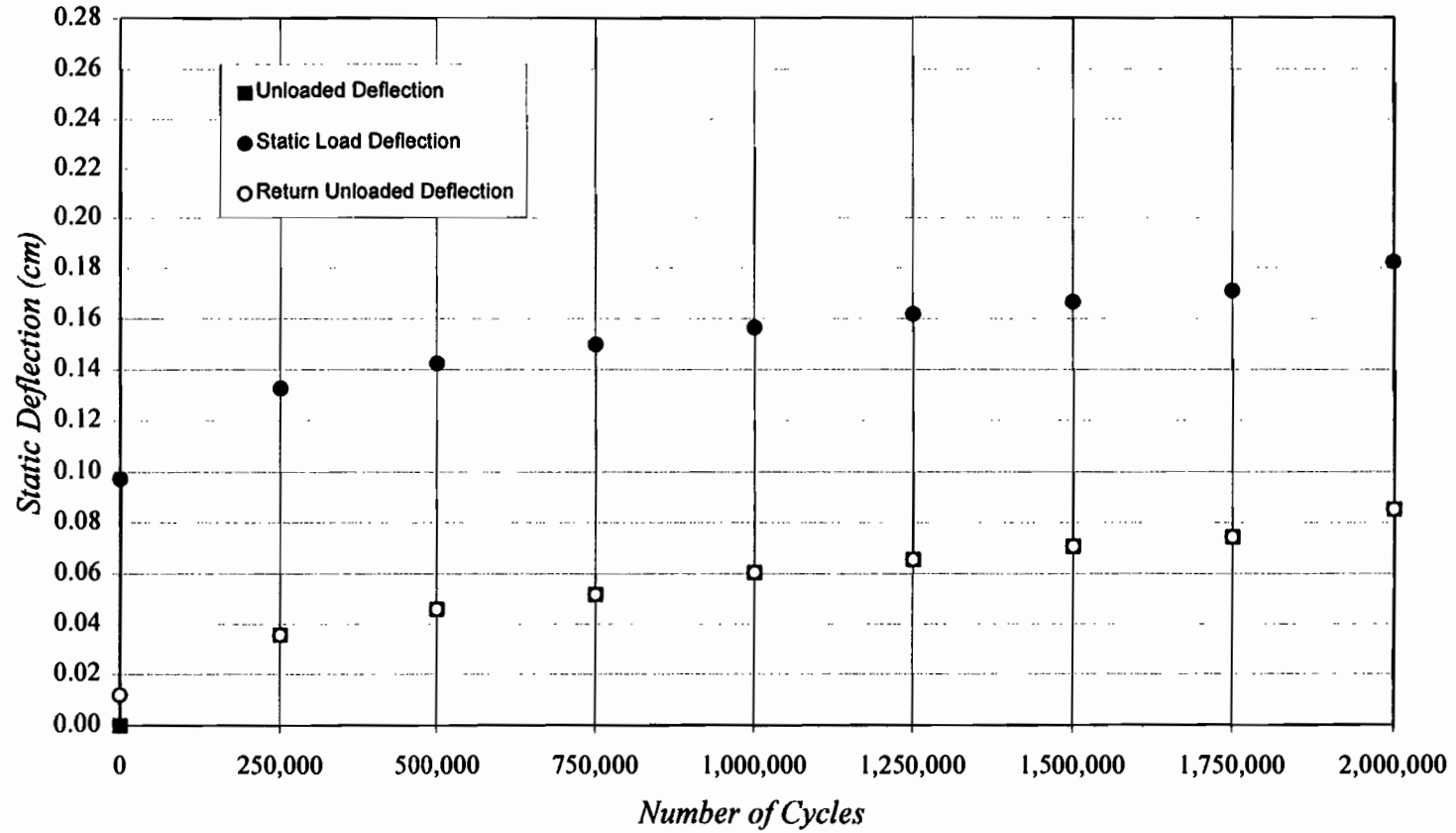


**Figure 7.2. Static Load Deflections For Fatigue Beam #2**  
**Initial Overlay Compressive Strength = 48,955 kPa**

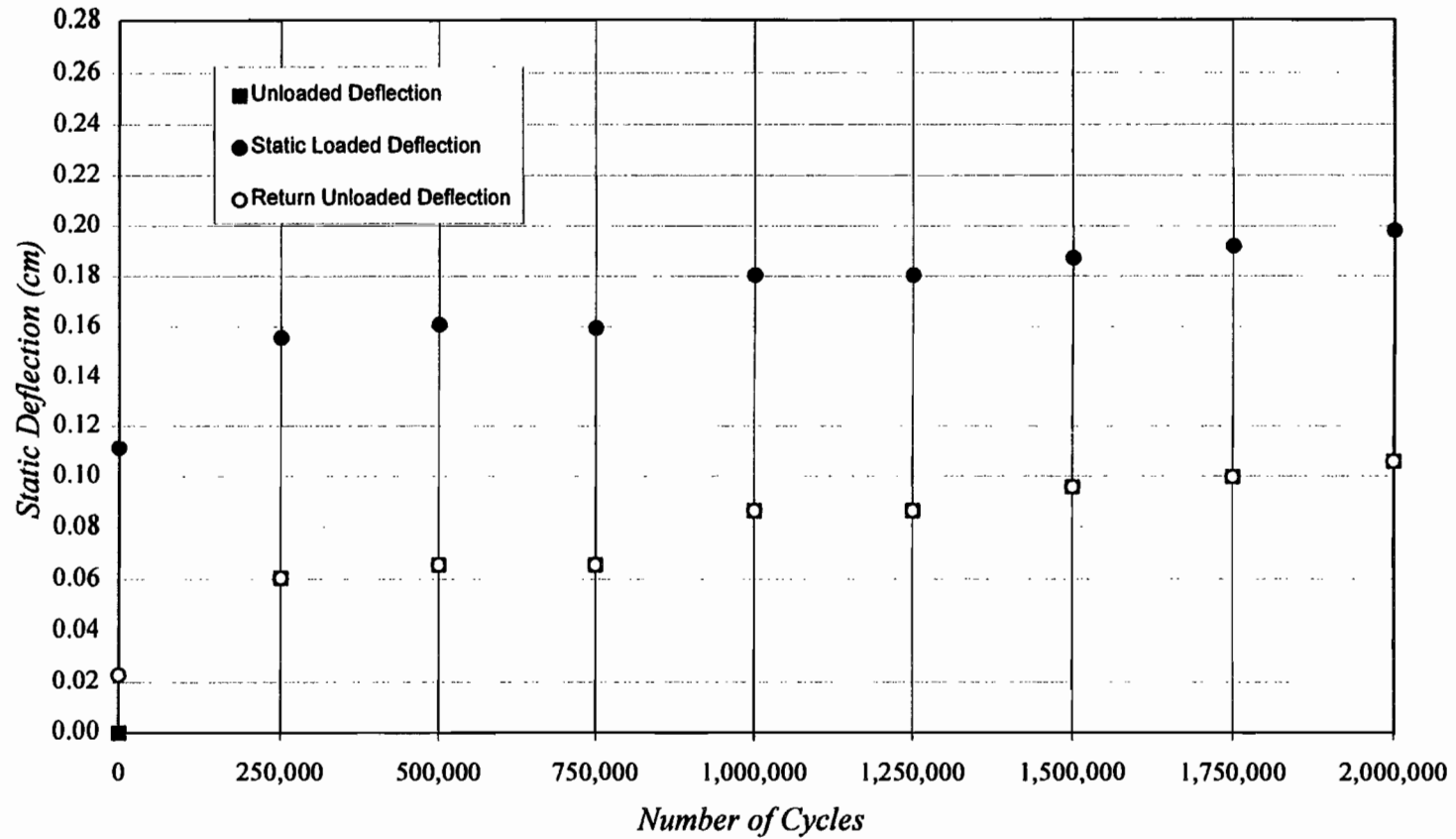


**Figure 7.3. Static Load Deflections For Fatigue Beam #3**  
**Initial Overlay Compressive Strength = 30,614 kPa**

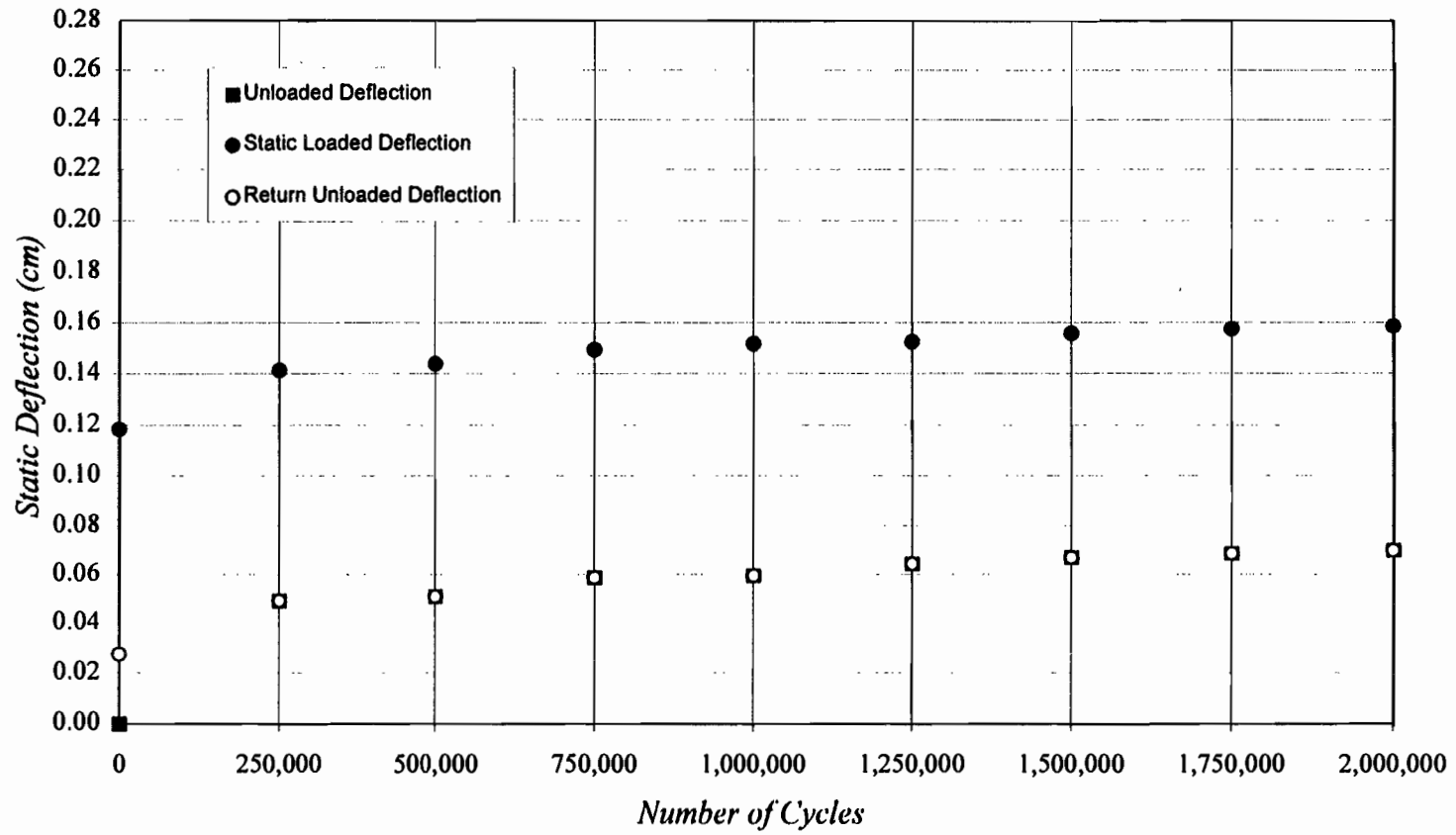


**Figure 7.4. Static Load Deflections For Fatigue Beam #4**  
**Initial Overlay Compressive Strength = 31,855 kPa**

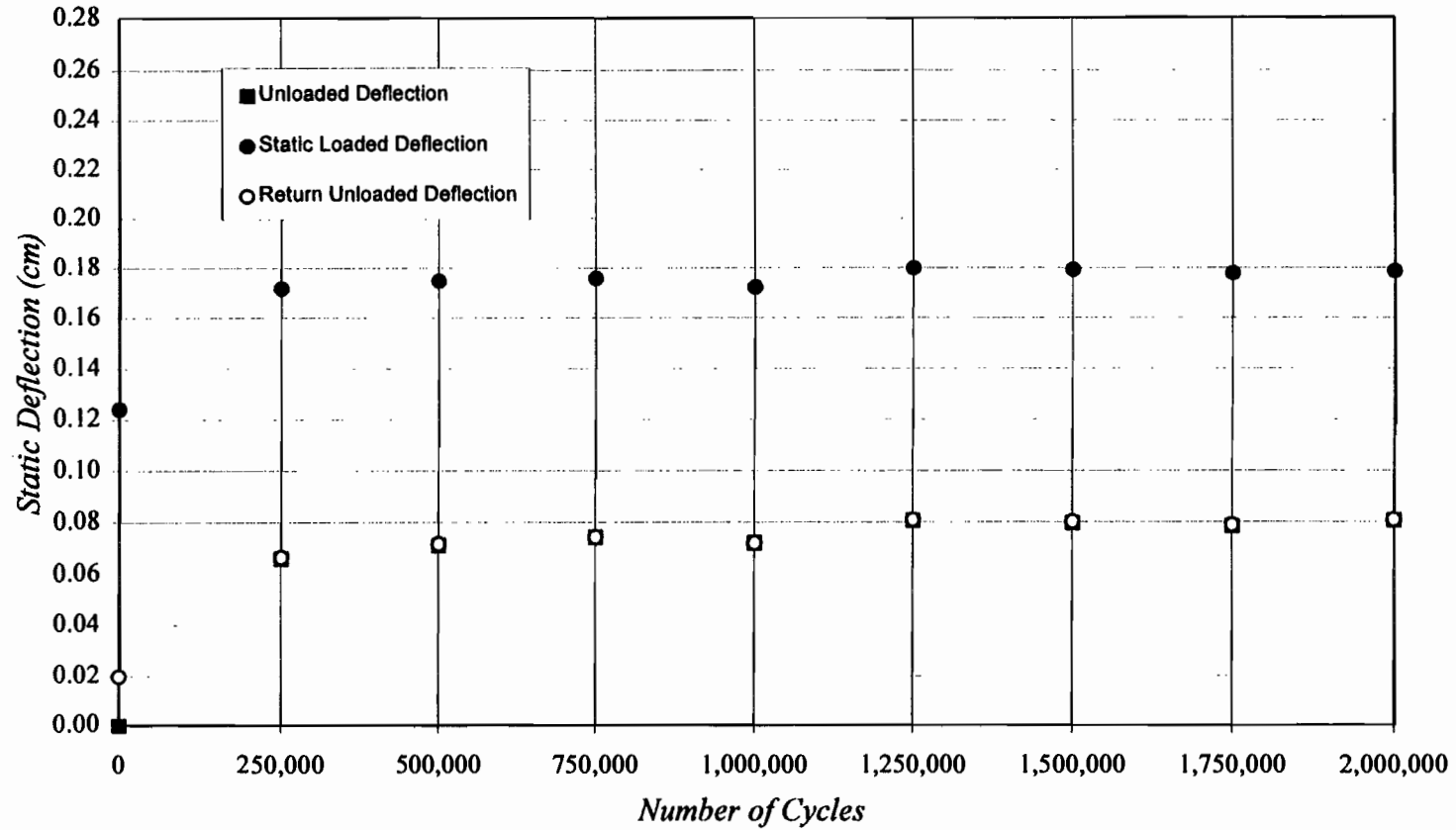


**Figure 7.5. Static Load Deflections For Fatigue Beam #5**  
**Initial Overlay Compressive Strength = 20,892 kPa**

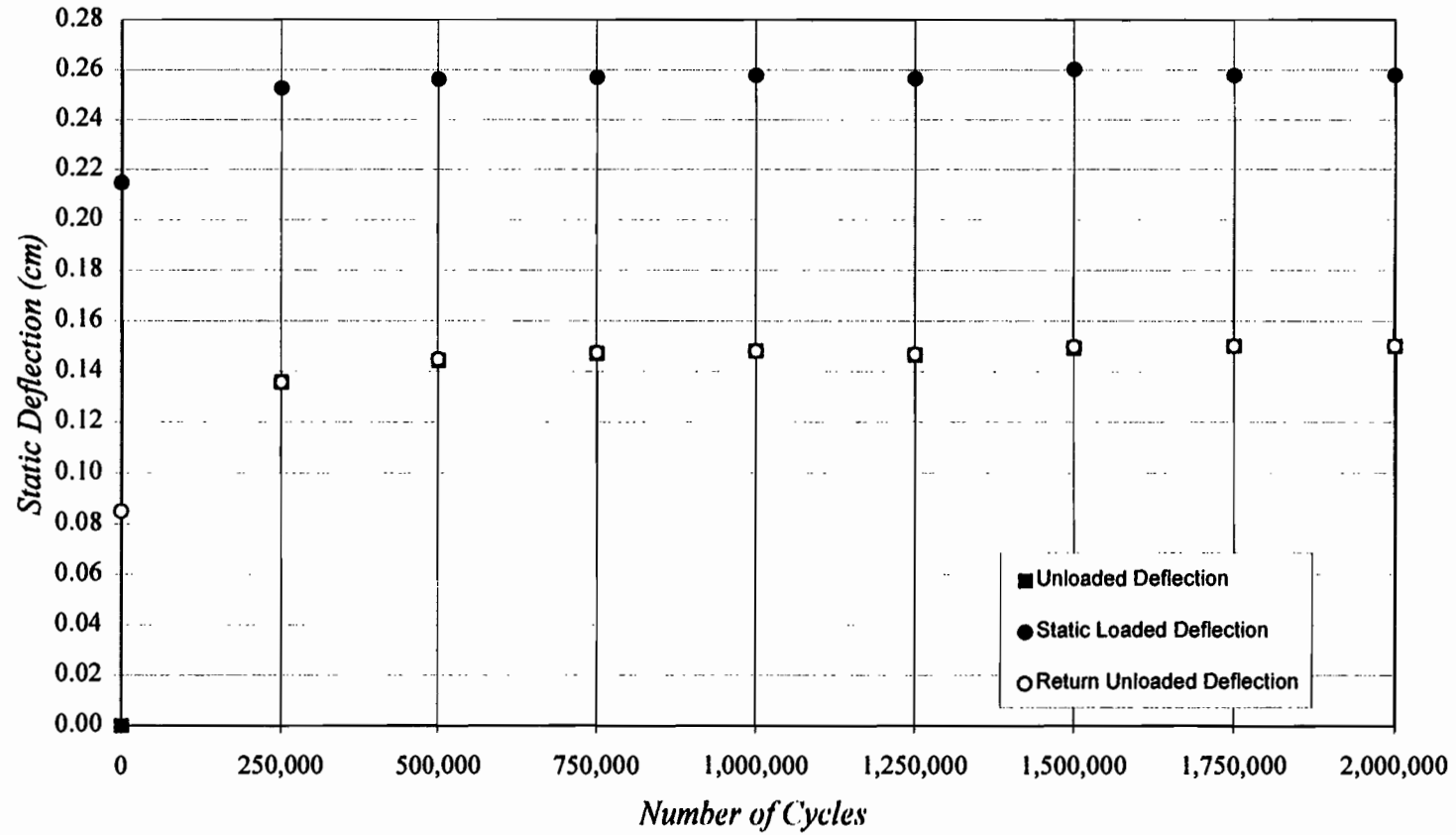


**Figure 7.6. Static Load Deflections For Fatigue Beam #6**  
**Initial Overlay Compressive Strength = 13,514 kPa**

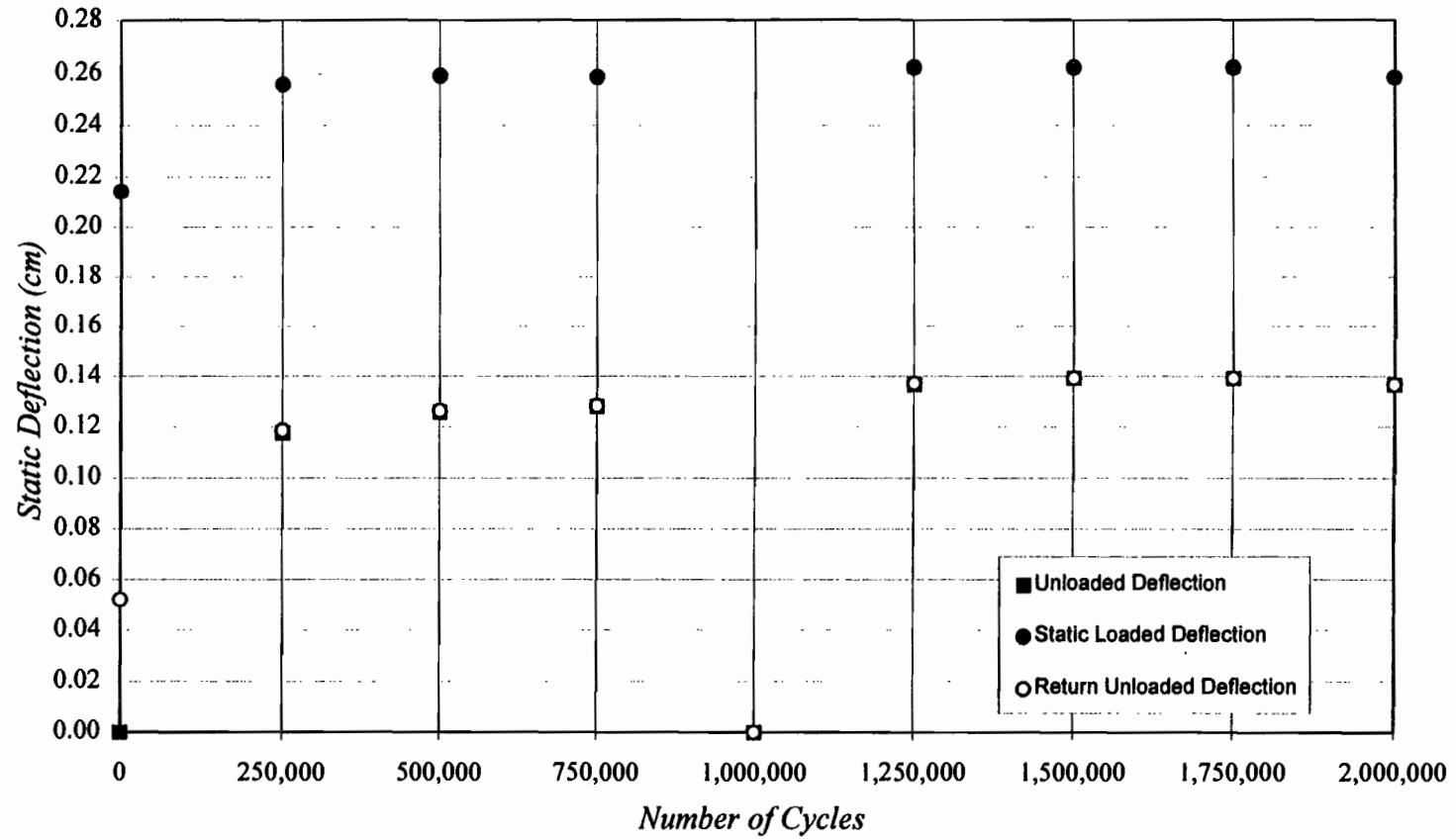


**Figure 7.7. Static Load Deflections For Fatigue Beam #7**  
**Initial Overlay Compressive Strength = 13,997 kPa**

**Table 7.1. Summary of Static Deflection Readings (cm)**

<b>Beam Specimen Number</b>	<b>Age at Fatigue Initiation</b>	<b>Strength at Fatigue Initiation (kPa)</b>	<b>Loaded Deflection Zero Cycles</b>	<b>Loaded Deflection 250,000 Cycles</b>	<b>Loaded Deflection 2,000,000 Cycles</b>	<b>Relative Deflection 250,000 Cycles</b>	<b>Relative Deflection 2,000,000 Cycles</b>
1	18 days	54,677	0.1074	0.1600	0.2042	0.1077	0.1074
2	9 days	48,955	0.0973	0.1326	0.1824	0.0968	0.0970
3	48 hours	30,627	0.1113	0.1557	0.1981	0.0953	0.0922
4	24 hours	31,834	0.1184	0.1412	0.1585	0.0919	0.0886
5	24 hours	20,921	0.1240	0.1717	0.1786	0.1057	0.0980
6	12 hours	13,494	0.2146	0.2527	0.2578	0.1171	0.1077
7	12 hours	13,996	0.2141	0.2560	0.2586	0.1384	0.1219

### **7.1.2 Beam Cracking**

The cracks occurring on the sides of each fatigue beam were marked and measured after each 250,000 load cycles. Drawings of the crack patterns and their progression during testing can be found in Appendix B. The appearance and progression of the beam cracks closely followed increases in deflection readings. A vast majority of the cracks occurred during the first full loading and after 250,000 load cycles. Beams one through three, which continued to experience increasing deflections during the entire testing program, had cracks which also grew in length and number as testing progressed. Cracks clustered at the bottom of the base beam near the loading head and extended up to thirty-five cm away. For the remaining beams, the growth of cracks generally ceased after 500,000 cycles. The crack line above the pre-cracked base beam location extended up into the overlay from 2.5 to 5.0 cm. Generally, no other cracks extended into the overlay.

### **7.2 DEVELOPMENT OF OVERLAY COMPRESSIVE STRENGTH**

Monitoring the continued development of overlay compressive strengths during fatigue testing was done to provide an additional benchmark for analysis of the fatigue testing results. Because beams #1 and #2 were fully cured when fatigue testing began, no additional cylinders were tested for compressive strength. These beams reached overlay strengths 54,677 kPa and 48,955 kPa at eighteen and nine days, respectively. For the remaining five beams, cylinders were tested periodically during the load cycling process. Figures 7.8 through 7.12 indicate how the overlay mix of beams three through seven continued to gain strength. The axis ordinates zero through eight, labeled “day of fatigue testing”, represent the day load cycling began and each subsequent twenty-four hour period at which 250,000 cycle interval deflection readings were taken. Testing of beam #3 began at an age of forty-eight hours when the overlay strength reached 30,627 kPa. A final strength of 39,150 kPa was achieved at the end of testing. Beam #4 cured more rapidly, reaching 31,834 kPa at twenty-four hours and 43,627 kPa by test’s end. Although beam #5 reached a similar strength of 44,581 kPa, the initial capacity of 20,921 kPa also took twenty-four hours to attain. Beams #6 and #7 reached their initial strengths of 13,494

kPa and 13,996 kPa at only twelve hours and attained strengths of 40,761 kPa and 35,816 kPa by the conclusion of testing.

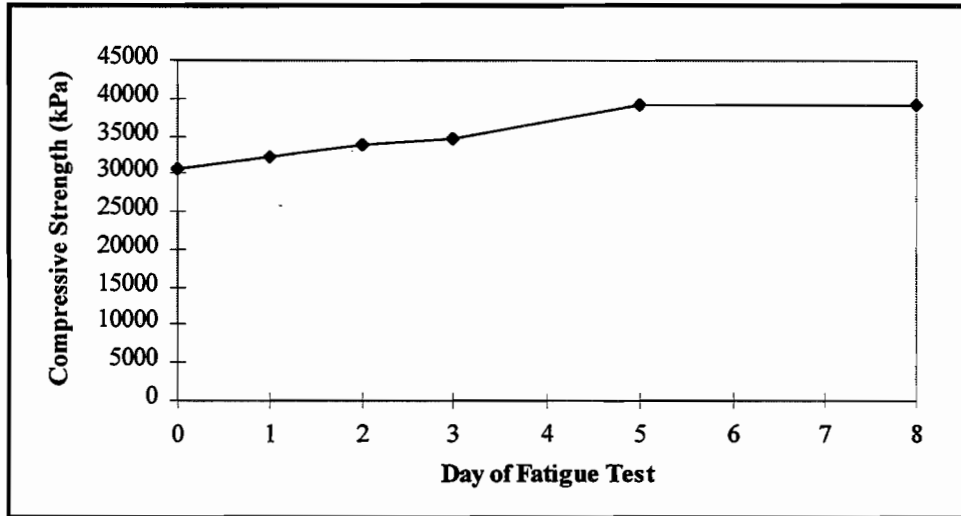


**Figure 7.8. Development of Beam #3 Overlay Compressive Strength, Age = 48 Hours at Fatigue Initiation**

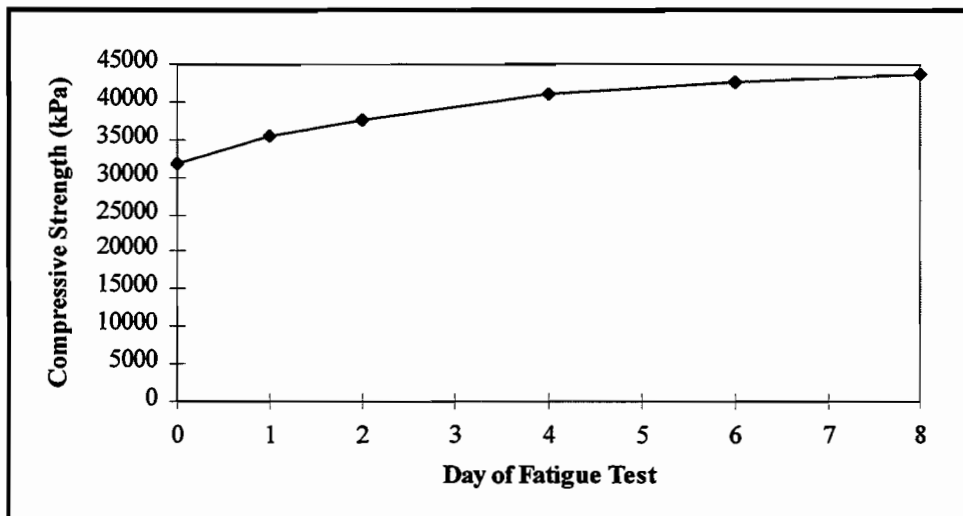


**Figure 7.9. Development of Beam #4 Overlay Compressive Strength, Age = 24 Hours at Fatigue Initiation**

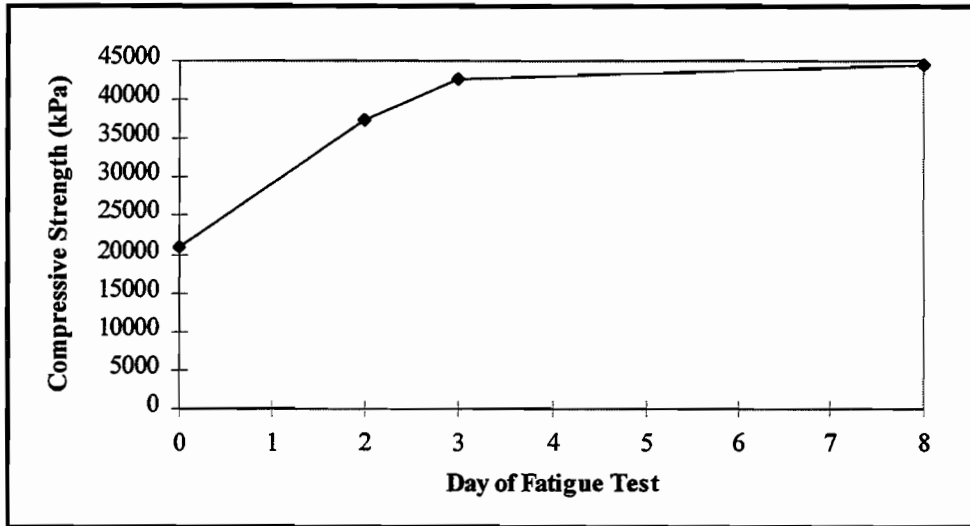


**Figure 7.10. Development of Beam #5 Overlay Compressive Strength, Age = 24 Hours at Fatigue Initiation**

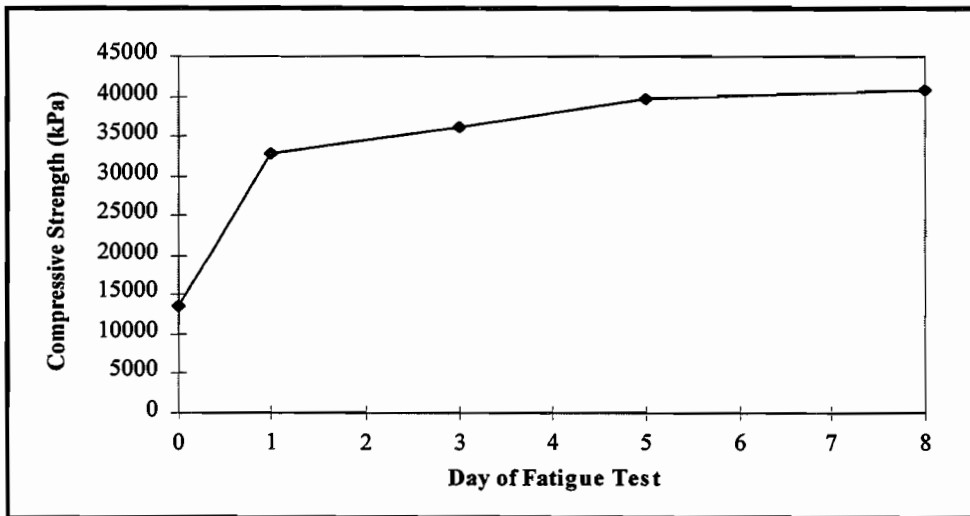


**Figure 7.11. Development of Beam #6 Overlay Compressive Strength, Age = 12 Hours at Fatigue Initiation**

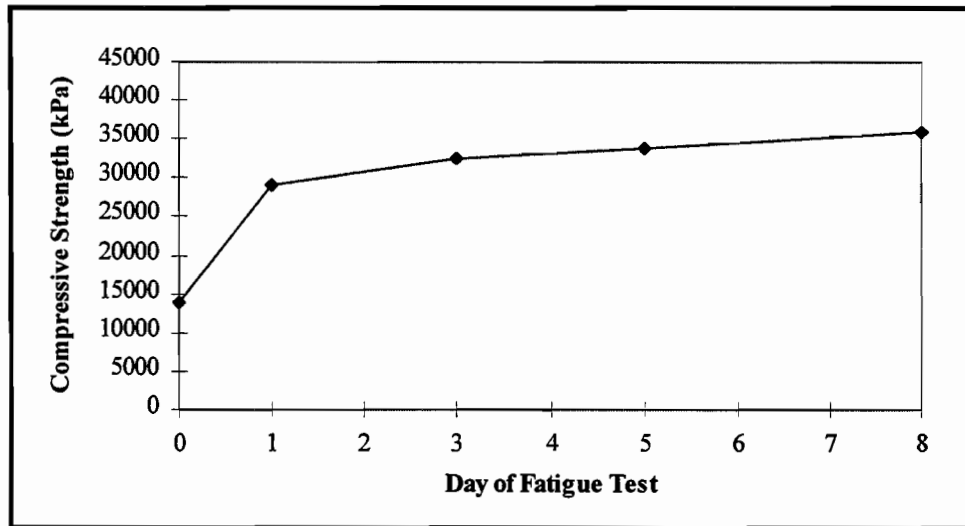


**Figure 7.12. Development of Beam #7 Overlay Compressive Strength, Age = 12 Hours at Fatigue Initiation**

### 7.3 INTERFACE BOND STRENGTH

Results from tests of interface bond strength of the fully cured beams are presented in table 7.2. The guillotine and direct tension methods were employed. The guillotine method produced significant variability in bond shear strengths of the full depth cores. While the extreme low value of 934 kPa can be attributed to damage from drilling through reinforcing steel, the remaining range of 2,635 kPa to 10,211 kPa is too large for reliable analysis. The interface shear strengths of cores three, five, and six do correlate well with the average strength of 3380 kPa from Wade. The values from cores one, four, and seven, however, fall well above expected shear capacity. It was noted after testing that these cores did not break cleanly at the interface. Portions of the base aggregate fractured off with the overlay.

Bond strength tests by the direct tension method produced more consistent and reliable results. The low value of 878 kPa from beam #4 can be attributed to poor base shotblasting at the beam end. The overlay pulled cleanly from the base. Subsequent inspection revealed that the laitance paste of the base beam had not been fully removed during the base preparation process. The remaining six partial depth cores pulled off at tension values between 1,372 kPa and 2,032 kPa. Cores from beams three, five, and six fractured in the base aggregate 1.0 to 2.0 cm below

the interface. Beam Core two separated cleanly at the interface, while beam core one partially fractured the base concrete and partially separated cleanly at the interface. The final core, from beam seven, fractured 1.5 cm from the top of the overlay.

**Table 7.2. Interface Bond Strength Of Fully Cured Overlay Beams**

<b>Beam Specimen Number</b>	<b>Guillotine Shear Strength (kPa)</b>	<b>Direct Tension Strength (kPa)</b>
1	7,086	1,372
2	934	1,757
3	4,090	2,032
4	6,533	878
5	4,282	2,032
6	2,635	1,647
7	10,211	1,372

## CHAPTER EIGHT: ANALYSIS OF RESULTS

### 8.1 EFFECTS OF EARLY AGE LOADING

Results of the early age fatigue testing program indicate that the bonded concrete overlay is less susceptible to early traffic loading than anticipated. Because beams #3 and #4 did not show clear signs of deteriorating behavior compared to the fully cured beams, the original testing schedule was revised. In addition to the moderate 31,000 kPa initial strength of these beams and the low 20,920 kPa initial strength of beam #5, an additional pair of very early age specimens was added to the program. These beams, #6 and #7, had an overlay compressive strength of 13,500 kPa at the start of fatigue testing. For further comparison, beam seven also contained a region of interface debond at midspan. The addition of these beams allowed for clearer insight into the response of the BCO to early age loading.

#### 8.1.1 Summary Of Behavior Trends

Two distinct trends emerged as beam specimens were subjected to fatigue loading at progressively earlier ages and lower overlay compressive strengths. These divergent trends are compared in Figure 8.1 using the static deflection graphs of beams #1 and #6. These two beams members are each representative of one particular trend in behavior.

Beam #1, shown with dashed lines, illustrates the behavior trend followed by beams #1 through #4. Overlays of these specimens were either fully or substantially cured at the beginning of fatigue testing (section 7.2). These beams experienced increasing levels of cracking and deflection throughout the testing process. The rate of increase of loaded deflections was high during the first 1,000,000 cycles then tapered off to nearly zero by 2,000,000 cycles. The total increase in static deflections during testing was approximately one hundred percent. The relative deflection range, between unloaded and loaded deflection curves, remained constant.

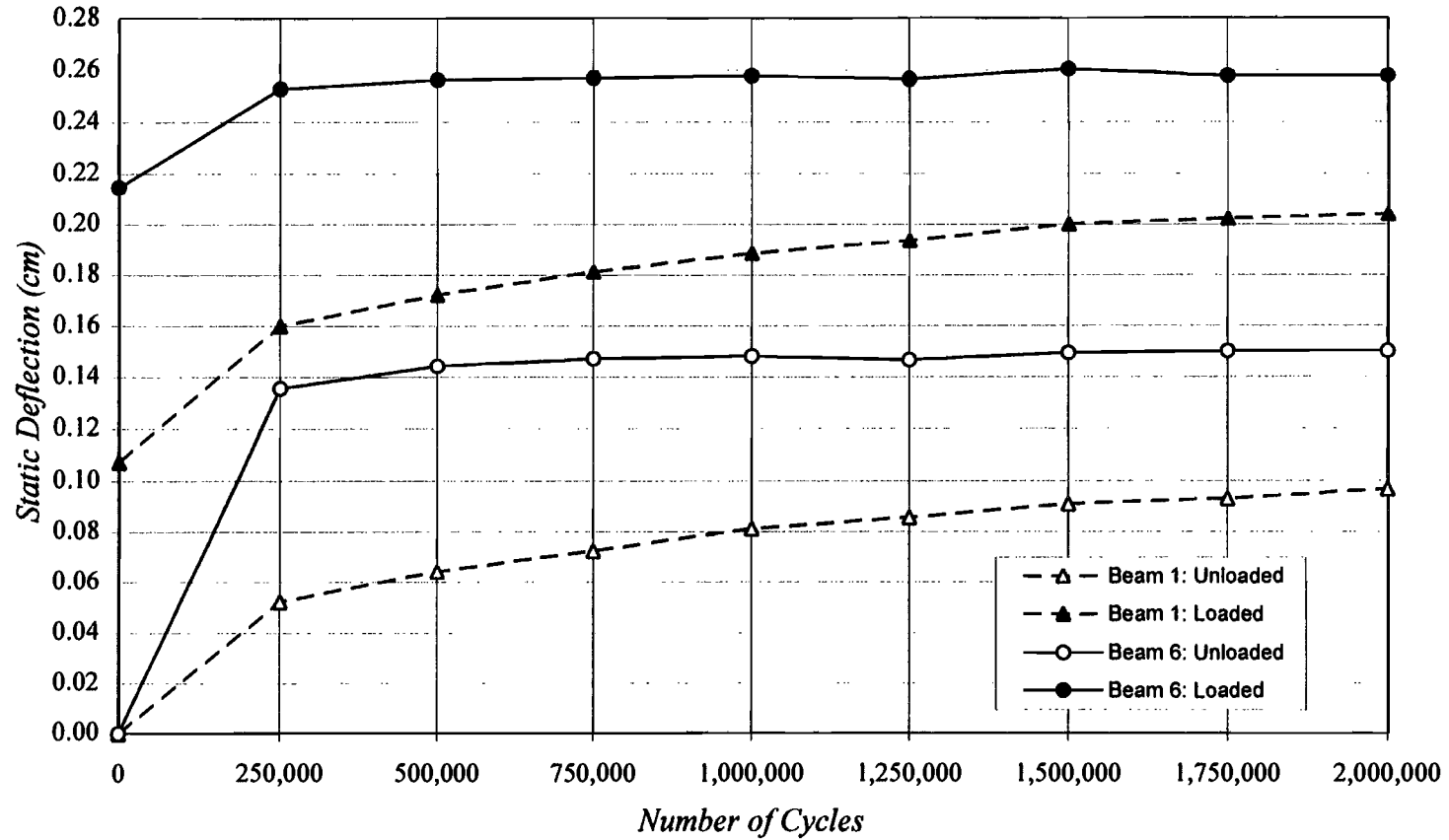


**Figure 8.1. Divergent Trends In Static Load Deflections  
(Fatigue Beams #1 And #6)**

Beam #6, shown with solid lines, typifies the trend in behavior followed by beams #5, #6, and #7. Fatigue testing of these members began less than twenty-four hours after overlay casting while rapid strength gain was still occurring. These beams underwent substantially larger deflections under the static load prior to initiation of load cycling. Large deflection increases occurred only during the first 250,000 cycles. After this, loaded deflection readings remained essentially constant. The total increase during 2,000,000 load cycles amounted to only twenty percent. The relative deflection range, however, did decrease by ten percent during the course of testing (Table 7.1). In effect, the unloaded deflection curve increased slightly while the loaded curve remained constant.

In Figures 8.2 and 8.3, relative static beam deflections are plotted as a function of overlay modulus for beams #5 and #6. Both graphs reveal a linear trend in decreasing relative deflections with increasing overlay modulus. Beam #6, tested at a lower initial overlay stiffness, decreased deflections at a sharper rate, but final values were still higher than beam #5.

Two final important observations can be made. First, the debonded region of beam #7 had no discernible effect on behavior or deflections. Second, despite the fact that fatigue testing of beam #6 began with an overlay compressive strength of only 13,500 kPa, the final static deflection readings were at most forty percent higher than those of fully cured beams.

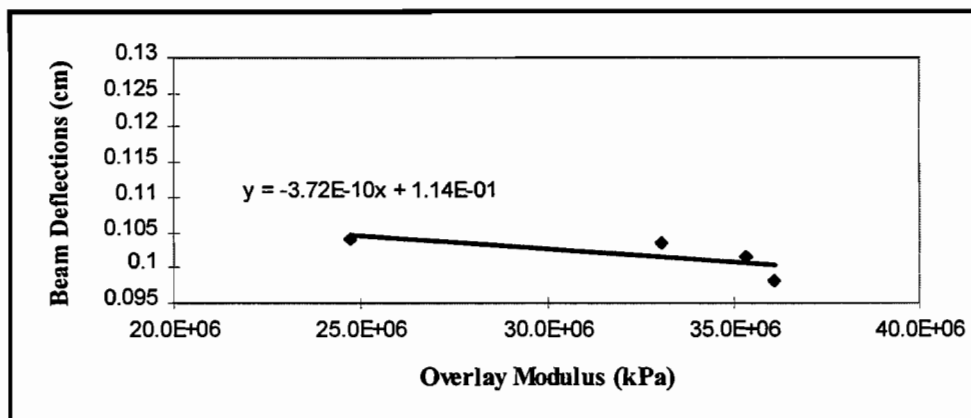


**Figure 8.2. Beam #5 Static Deflections vs. Overlay Modulus**

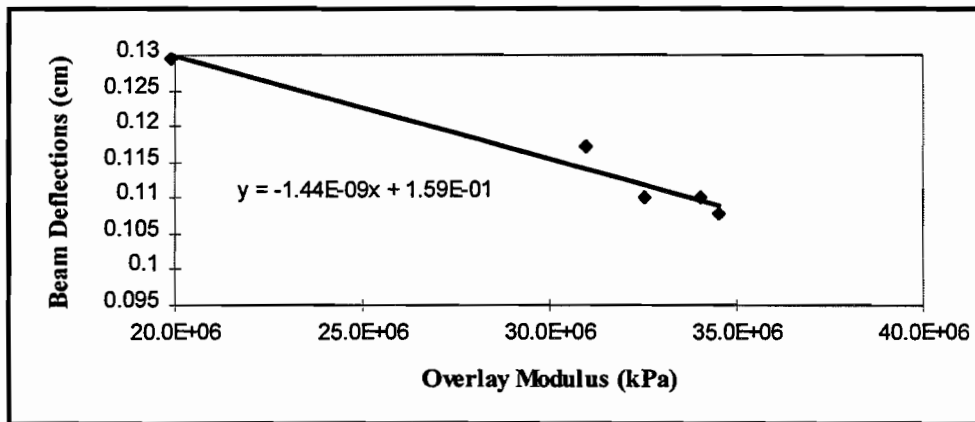


**Figure 8.3. Beam #6 Static Deflections vs. Overlay Modulus**

### 8.1.2 Prediction of Deflections

An attempt to predict the relative beam deflections by ACI 318 section 9.5.2.3 was largely unsuccessful (Ref 23). In this method, deflections were calculated with an effective moment of inertia that attempted to account for cracking along the beam length. The overlay was transformed to an equivalent width such that the entire beam calculation relied on the base beam stiffness of  $28.3 \times 10^6$  kPa. At twelve hours beam #6 had an overlay strength of 13,500 kPa and stiffness of  $19.7 \times 10^6$  kPa. The effective moment of inertia was  $7,770 \text{ cm}^4$  compared to a gross inertia of  $12,487 \text{ cm}^4$ . Based on this value, the deflection was 0.061 cm. The actual measured deflection of 0.127 cm was 108% larger. Calculations of deflections at other overlay strengths showed similar discrepancies. The ACI method of calculating beam deflections did not predict the actual because the effective moment of inertia formula does not account for composite beams with varying overlay stiffnesses.

### 8.1.2 Analysis

The two distinct trends which appeared during the fatigue testing program were unanticipated. Beams #5, #6, and #7, with very young overlays, were expected to follow a trendline similar to beams #1 through #4. Their initial deflections would have been larger due to the low overlay stiffness, and the increase in deflections throughout testing would have been

larger due to damage from early loading. Since this second effect obviously did not happen, a re-analysis of the behavior was necessary.

For beams #1 through #4, the continued increase in loaded deflection readings was due to progressive cracking caused by fatigue loading damage. As the number and length of cracks grew with additional cycles (Appendix B) the beams developed a permanent deflection offset in the unloaded position. This can be seen in the open triangle - dashed line of Figure 8.1. Since the relative deflection range did not change, the loaded deflection curve followed this same trend of increases.

With beams #5, #6, and #7, beam cracking effectively ceased to progress after 250,000 cycles. The corresponding permanent deflection offset is shown in the open circle - solid line of Figure 8.1. Between 250,000 and 2,000,000 cycles additional cracking was negligible and the unloaded permanent offset increased only slightly. Because the relative deflection was gradually decreasing due to the stiffening overlay, the net result was a nearly constant loaded deflection curve.

Variations in behavior between the cured and fresh overlay beams involve the strength gain rate of the overlay mix. As Figures 7.10 through 7.12 show, compressive strengths of the overlays increased very rapidly during the first twenty-four hours of testing. While cracking damage occurred during this brief period, little happened afterwards. Effectively, a balance was reached between fatigue damage and strength resistance. Instead of undergoing damage throughout the entire 2,000,000 cycles of testing, the early age beams experienced the cumulative fatigue effects during the first twenty-four hours while strength was still relatively low. Beyond 250,000 cycles, when the overlay had reached a substantial fraction of final strength, the deflection curves of these beams flatten out in a manner similar to the cured beams' deflection curves past 1,500,000 cycles. The total fatigue damage was 'front-loaded' for these members.

An additional reason behind the lack of continued damage involves the phenomenon known as autogenous healing of concrete (Ref 22). During the first four days of testing, substantial concrete hydration and strength gain continued in the overlays. The developing matrix of hydration products within the overlay arrested or even healed microcrack damage. As

hydration proceeds, this matrix extends outwards to form a tighter 'mesh' which envelops microcracks and stops them from extending further into the overlay. Since the major base beam cracking had already transpired, re-sealing the overlay microcracks would serve to halt any further deflection offset of the test specimen.

## **8.2 INTERFACE BOND**

While results of the guillotine bond test were somewhat erratic, the average interface shear strength of 3,670 kPa for beams #3, #5, and #6 correlates well with the 3,380 kPa average strength measured by Wade. The direct tension test produced more consistent results with an average tensile bond strength of 1,584 kPa. Both values greatly exceed the maximum theoretical stress of 496 kPa established by earlier research (5). This nominal stress value includes the combined effects from concrete shrinkage, thermal gradients, and traffic loading.

During fatigue testing of overlay beam specimens #1 through #6, no interface delaminations occurred. This was verified visually by inspection of crack patterns and widths on the side of each beam. Beam #7, with the debonded central section, did not experience any spreading of the debonded region. This was verified both visually and through sounding with a hammer. Corroboration of non-debonding comes from the fact that the overlay did not separate from the base during coring. If debonding had occurred, the overlay portion of the core would have detached and lodged inside the core barrel.

Both observations of interface bond strength and lack of debonding indicate that sufficient bond was achieved between the base beams and overlays. Moderate shotblasting of the base surface, as described in chapter five, provides adequate texture for interlock with the overlay mix.

## **CHAPTER NINE: SUMMARY, CONCLUSIONS, AND RECOMMENDATIONS**

### **9.1 SUMMARY**

In order to determine the effects of early age loading on the IH-10 bonded concrete overlay pavement in El Paso, a laboratory fatigue testing program was developed. Seven beams were made and loaded on simple supports. The half-scale specimens consisted of 10.16-cm-thick reinforced base beams overlaid with 7.62-cm of high strength concrete mix. Base concrete simulated the existing IH-10 pavement and the overlay mix was designed specifically for the BCO project.

The composite beams were fatigue loaded at sixty-five percent of their flexural capacity. The applied loading of 18,245 N exceeded the half-scale equivalent single axle load (ESAL) of 11,120 N by sixty-five percent. While actual El Paso traffic volumes account for only 5,000,000 single axle loads in a one-year period, the loading rate of three Hertz produced 2,000,000 load cycles in eight days. Deflection and crack readings were taken at 250,000 cycle intervals throughout testing. By varying the initial overlay strength from 13,500 kPa to 48,500 kPa, trends in beam response to early age loading were observed and analyzed.

### **9.2 CONCLUSIONS FROM FATIGUE PROGRAM**

After a complete analysis of results from the fatigue testing program, a number of conclusions can be drawn concerning early traffic loading on a bonded concrete overlay. The most important conclusion is that expedited paving of the BCO is feasible without causing long-term damage to the pavement. An evaluation of the interface bonding is also possible. While the fatigue testing procedure utilized precludes making a direct comparison of project results with the actual El Paso pavement, sufficiently strong trends developed to allow correlation of fatigue beam behavior to pavement behavior.

#### **9.2.1 Early Age Loading**

1. Bonded overlay beams endured early age loading with little more effect than fully cured specimens.

2. Young beams experienced higher initial damage (cracking and deflections) during the first twenty-four hours of testing.
3. Rapid strength and stiffness gains in the overlay concrete halted the progression of fatigue damage in young beams after twenty-four hours.
4. Final deflections of young beams were at most forty percent larger than those of beams with fully cured overlays at loading initiation.
5. Beam cracking of all specimens at test conclusion compared quite similarly.
6. Early age loading effects were minimal when considering that young beams had an overlay strength of 13,500 kPa at fatigue initiation compared to the fully cured beams' overlay strength of 48,265 kPa.

### **9.2.2 Interface Bond**

1. Lack of debonding during fatigue testing of the beams indicates that the interface acquired sufficient bond strength at early ages to withstand stresses from loading, shrinkage, and thermal variance.
2. The average fully cured interface bond strengths of 3,380 kPa in shear and 1,583 kPa in tension both exceed the maximum calculated pavement stress of 496 kPa.
3. Due to similarities in base preparation methods and concrete mix strengths, the bond results should closely match those for the actual pavement

### **9.3 RECOMMENDATIONS**

1. Results of this fatigue testing program reveal that traffic flow can be allowed on IH-10 within twelve hours after placing the overlay concrete.
2. Because the extreme summer weather of El Paso could cause shrinkage and thermal effects not seen in the laboratory, a full-scale test section should be constructed to verify results.
3. If further testing reveals additional damage due to extreme weather conditions, methods of reducing shrinkage and thermal effects during the overlay's first twenty-four hours should be investigated and implemented.
4. Until further testing verifies the results of this program, the overlay concrete should cure for twenty-four hours before the application of full traffic.

## REFERENCES

1. Allison, Brent T., McCullough, B. Frank, and Fowler, David W., "Feasibility Study for a Full-Scale Bonded Concrete Overlay on IH-10 in El Paso, Texas," Research Report 1957-1F, Center for Transportation Research, The University of Texas at Austin, January 1993.
2. Whiting, D., et al., "Synthesis of Current and Projected Concrete Highway Technology," SHRP-C-345, Strategic Highway Research Program, National Research Council, Washington D.C., August 1993.
3. Lundy, James R., McCullough, B. Frank, and Fowler, David W., "Delamination of Bonded Concrete Overlays at Early Ages," Research Report 1205-2, Center for Transportation Research, The University of Texas at Austin, January 1991.
4. Bagate, Moussa, McCullough, B. Frank, and Fowler, David W., "An Experimental Thin-Bonded Concrete Overlay Pavement," Research Report 357-2F, Center for Transportation Research, The University of Texas at Austin, November 1985.
5. Teo, Kok Jin, Fowler, David W., and McCullough, B. Frank, "Monitoring and Testing of the Bonded Concrete Overlay on IH-610 in Houston, Texas," Research Report 920-3, Center for Transportation Research, The University of Texas at Austin, February 1989.
6. Whitney, David P., Isis, Polykarpos, McCullough, B. Frank, and Fowler, David W., "An Investigation of Various Factors Affecting Bond in Bonded Concrete Overlays," Research Report 920-5, Center for Transportation Research, The University of Texas at Austin, June 1992.
7. Kailasanathan, Kandiah, McCullough, B. Frank, and Fowler, David W., "A Study of the Effects of Interface Condition on Thin Bonded PCC Overlays," Research Report 357-1, Center for Transportation Research, The University of Texas at Austin, December 1984.
8. Delatte, Norb , Fowler, David W., and McCullough, B. Frank, "Full Scale Test of High Early Strength Bonded Concrete Overlay Designs and Construction Methods," Transportation Research Board, paper presented for publication, July 1995.
9. "Fast Track Overlays," Concrete Construction, Volume 35, December 1990.
10. van Metzinger, Willem A., McCullough, B. Frank, and Fowler, David W., "An Empirical-Mechanistic Design Method Using Bonded Concrete Overlays for the Rehabilitation of Pavements," Research Report 1205-1, Center for Transportation Research, The University of Texas at Austin, January 1991.

11. van Metzinger, Willem A., Lundy, James R., McCullough, B. Frank, and Fowler, David W., "Design and Construction of Bonded Concrete Overlays," Research Report 1205-4F, Center for Transportation Research, The University of Texas at Austin, January 1991.
12. Wade, Dawn M., Fowler, David W., and McCullough, B. Frank, "Concrete Bond Characteristics for a Bonded Concrete Overlay on IH-10 in El Paso," Research Report 2911-2, Center for Transportation Research, The University of Texas at Austin, July 1995.
13. Reilley, Karen, Saraf, Chhote, McCullough, Frank B., and Fowler, David W., "A Laboratory Study of the Fatigue of Bonded PCC Overlays," Research Report 457-2, Center for Transportation Research, The University of Texas at Austin, September 1986.
14. "ACI 211, 1-81 Standard Practice for Selecting Proportions for Normal, Heavyweight, and Mass Concrete," American Concrete Institute, 1980.
15. "Standard Specifications for Construction of Highways, Streets, and Bridges," Texas Department of Transportation, 1993.
16. Kosmatka, S. H. and Panarese, W. C., Design and Control of Concrete Mixtures, Portland Cement Association, 13<sup>th</sup> Edition, Skokie, Illinois, 1992.
17. American Society for Testing Materials, 1994 Annual Book of ASTM Standards, volume 04.02, Concrete and Aggregates.
18. Mindess, Sidney and Young, J. Francis, Concrete, Prentice and Hall Inc., Engelwood Cliffs, New Jersey, 1981.
19. Choi, Dong Uk, Shear Block Test Method, The University of Texas at Austin, 1994.
20. King, William M., "Design and Construction of a Bonded Fiber Concrete Overlay of CRCP," Louisiana Transportation Research Center, January 1992.
21. Rasmussen, Robert O., "Determination of Overlay Thickness," Technical Memorandum 2911-9, Center for Transportation Research, The University of Texas at Austin, 1994.
22. Neville, A. M., Properties of Concrete, Pitman Publishing Limited, 3<sup>rd</sup> Edition, London, 1981.
23. Building Code Requirements for Reinforced Concrete (ACI 318-89), American Concrete Institute, Detroit, Michigan, 1989.

## **APPENDIX A: BEAM DEFLECTION DATA**



<b>Fatigue Beam Cyclic Testing Data</b>					
<b>BEAM 1: Overlay cured to 54,677 kPa</b>					
test date: 1/31/95 to 2/8/95					
<b>Static Deflection Readings Under 18,245 N loading</b>					
counter	initial	deflected	return		difference
0	0.0000	0.1074	0.0122		0.1074
250,000	0.0523	0.1600	0.0523		0.1077
500,000	0.0643	0.1722	0.0643		0.1080
750,000	0.0726	0.1814	0.0726		0.1087
1,000,000	0.0813	0.1887	0.0813		0.1074
1,250,000	0.0856	0.1938	0.0856		0.1082
1,500,000	0.0909	0.2002	0.0909		0.1092
1,750,000	0.0930	0.2024	0.0930		0.1095
2,000,000	0.0968	0.2042	0.0968		0.1074
<b>BEAM 2: Overlay cured to 48,955 kPa</b>					
test date: 2/11/95 to 2/19/95					
<b>Static Deflection Readings Under 18,245 N loading</b>					
counter	initial	deflected	return		difference
0	0.0000	0.0973	0.0117		0.0973
250,000	0.0358	0.1326	0.0358		0.0968
500,000	0.0460	0.1425	0.0460		0.0965
750,000	0.0518	0.1499	0.0518		0.0980
1,000,000	0.0605	0.1565	0.0605		0.0960
1,250,000	0.0655	0.1618	0.0655		0.0963
1,500,000	0.0706	0.1666	0.0706		0.0960
1,750,000	0.0744	0.1709	0.0744		0.0965
2,000,000	0.0853	0.1824	0.0853		0.0970

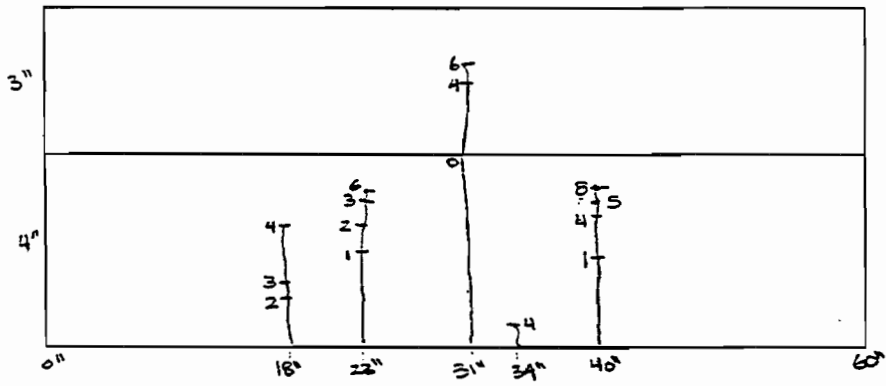
<b>Fatigue Beam Cyclic Testing Data</b>				
<b>BEAM 3: Overlay cured to 30,614 kPa</b>				
test date: 3/11/95 to 3/19/95				
Static Deflection Readings Under 18,245 N loading				
counter	initial	deflected	return	difference
0	0.0000	0.1113	0.0229	0.1113
250,000	0.0605	0.1557	0.0605	0.0953
500,000	0.0655	0.1608	0.0655	0.0953
750,000	0.0655	0.1595	0.0655	0.0940
1,000,000	0.0864	0.1803	0.0864	0.0940
1,250,000	0.0864	0.1803	0.0864	0.0940
1,500,000	0.0958	0.1872	0.0958	0.0914
1,750,000	0.0998	0.1920	0.0998	0.0922
2,000,000	0.1059	0.1981	0.1059	0.0922
<b>BEAM 4: Overlay cured to 31,855 kPa</b>				
test date: 3/20/95 to 3/28/95				
Static Deflection Readings Under 18,245 N loading				
counter	initial	deflected	return	difference
0	0.0000	0.1184	0.0274	0.1184
250,000	0.0493	0.1412	0.0493	0.0919
500,000	0.0511	0.1438	0.0511	0.0927
750,000	0.0587	0.1494	0.0587	0.0907
1,000,000	0.0594	0.1516	0.0594	0.0922
1,250,000	0.0643	0.1524	0.0643	0.0881
1,500,000	0.0668	0.1557	0.0668	0.0889
1,750,000	0.0686	0.1575	0.0686	0.0889
2,000,000	0.0699	0.1585	0.0699	0.0886

<b>Fatigue Beam Cyclic Testing Data</b>				
<b>BEAM 5: Overlay cured to 20,892 kPa</b>				
test date: 4/18/95 to 4/26/95				
<b>Static Deflection Readings Under 18,245 N loading</b>				
counter	initial	deflected	return	difference
0	0.0000	0.1240	0.0198	0.1240
250,000	0.0660	0.1717	0.0665	0.1057
500,000	0.0711	0.1748	0.0716	0.1036
750,000	0.0742	0.1758	0.0742	0.1016
1,000,000	0.0719	0.1722	0.0719	0.1003
1,250,000	0.0805	0.1798	0.0808	0.0993
1,500,000	0.0795	0.1793	0.0800	0.0998
1,750,000	0.0782	0.1778	0.0787	0.0996
2,000,000	0.0805	0.1786	0.0808	0.0980
<b>BEAM 6: Overlay cured to 13,514 kPa</b>				
test date: 5/08/95 to 5/16/95				
<b>Static Deflection Readings Under 18,245 N</b>				
counter	initial	deflected	return	difference
0	0.0000	0.2146	0.0851	0.2146
250,000	0.1356	0.2527	0.1356	0.1171
500,000	0.1443	0.2563	0.1448	0.1120
750,000	0.1471	0.2570	0.1473	0.1100
1,000,000	0.1481	0.2578	0.1481	0.1097
1,250,000	0.1466	0.2565	0.1468	0.1100
1,500,000	0.1494	0.2604	0.1499	0.1110
1,750,000	0.1501	0.2578	0.1501	0.1077
2,000,000	0.1501	0.2578	0.1501	0.1077

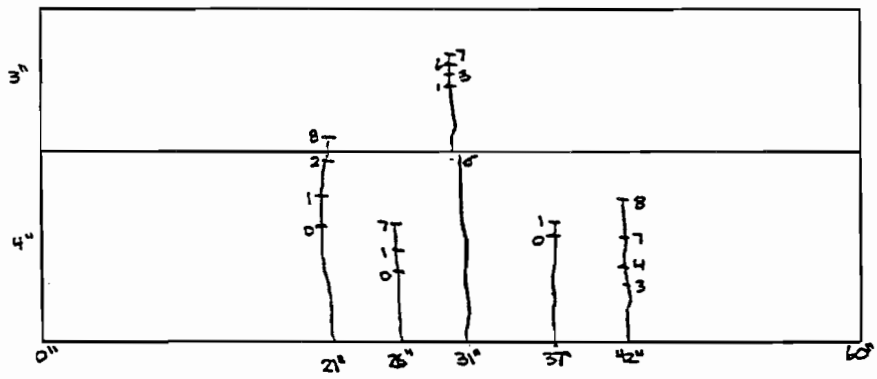
<b>Fatigue Beam Cyclic Testing Data</b>					
<b>BEAM 7: Overlay cured to 13,997 kPa - CENTRAL SECTION DEBONDED</b>					
test date: 5/23/95 to 5/31/95					
Static Deflection Readings Under 18,245 N loading					
counter	initial	deflected	return		difference
0	0.0000	0.2141	0.0521		0.2141
250,000	0.1176	0.2560	0.1186		0.1384
500,000	0.1257	0.2593	0.1262		0.1336
750,000	0.1280	0.2588	0.1283		0.1308
1,000,000	0.0000	0.0000	0.0000		0.0000
1,250,000	0.1367	0.2624	0.1372		0.1257
1,500,000	0.1392	0.2624	0.1392		0.1232
1,750,000	0.1392	0.2624	0.1392		0.1232
2,000,000	0.1367	0.2586	0.1367		0.1219

## **APPENDIX B: BEAM CRACKING**

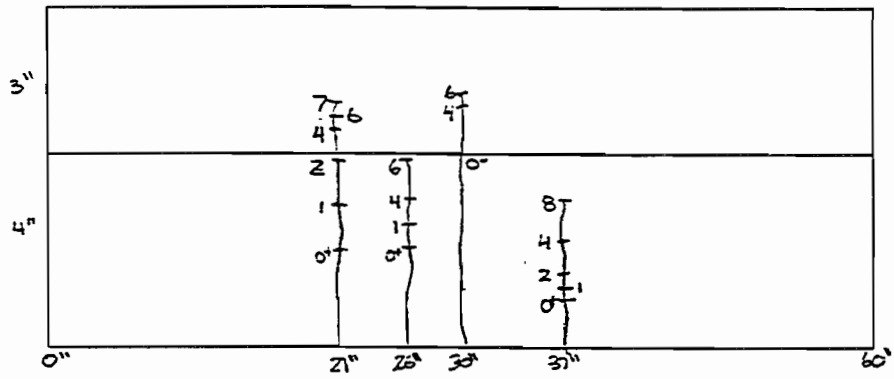




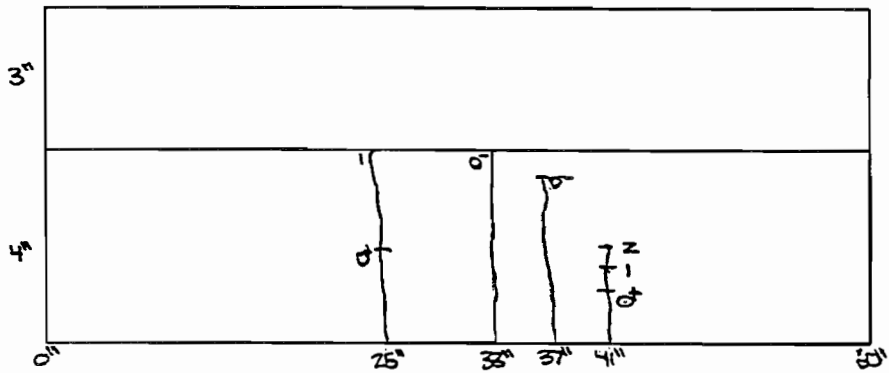
BEAM #1



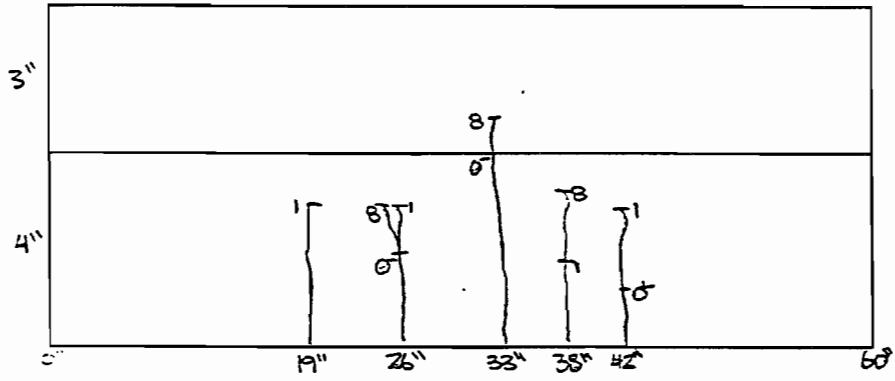
BEAM #2



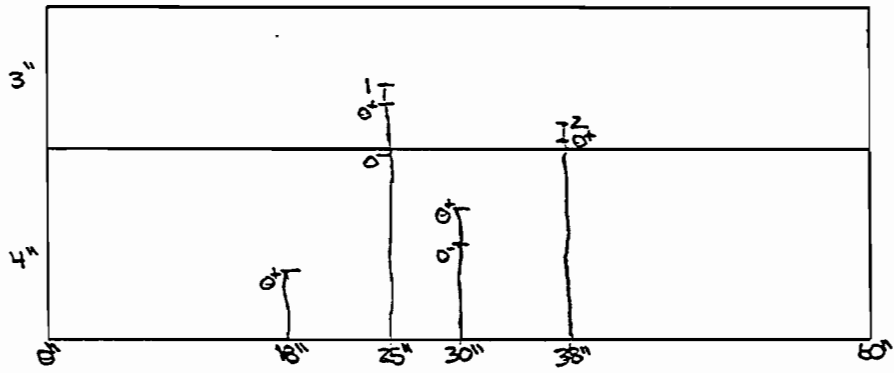
BEAM #3



BEAM #4



BEAM #5



BEAM #6